AD_____

Award Number: **W81XWH-10-1-0590**

TITLE: **Global Characterization of Protein-Altering Mutations in Prostate Cancer**

PRINCIPAL INVESTIGATOR: **Peter S. Nelson, M.D.**

CONTRACTING ORGANIZATION: **Fred Hutchinson Cancer Research Center**
Seattle, WA 98109-1024

REPORT DATE: **August 2013**

TYPE OF REPORT: **Final**

PREPARED FOR: U.S. Army Medical Research and Materiel Command
Fort Detrick, Maryland 21702-5012

DISTRIBUTION STATEMENT: Approved for Public Release;
Distribution Unlimited

REPORT DOCUMENTATION PAGE

Form Approved
OMB No. 0704-0188

1. REPORT DATE	2. REPORT TYPE	3. DATES COVERED
August 2013	Final	15 July 2010 – 14 July 2013

4. TITLE AND SUBTITLE
Global Characterization of Protein-Altering Mutations in Prostate Cancer

5a. CONTRACT NUMBER

5b. GRANT NUMBER
W81XWH-10-1-0590

5c. PROGRAM ELEMENT NUMBER

6. AUTHOR(S)
Peter S. Nelson

E-Mail: pnelson@fhcrc.org

5d. PROJECT NUMBER

5e. TASK NUMBER

5f. WORK UNIT NUMBER

7. PERFORMING ORGANIZATION NAME(S) AND ADDRESS(ES)
Fred Hutchinson Cancer Research Center
Seattle, WA 98109-1024

8. PERFORMING ORGANIZATION REPORT NUMBER

9. SPONSORING / MONITORING AGENCY NAME(S) AND ADDRESS(ES)
U.S. Army Medical Research and Materiel Command
Fort Detrick, Maryland 21702-5012

10. SPONSOR/MONITOR'S ACRONYM(S)

11. SPONSOR/MONITOR'S REPORT NUMBER(S)

12. DISTRIBUTION / AVAILABILITY STATEMENT
Approved for Public Release; Distribution Unlimited

13. SUPPLEMENTARY NOTES

14. ABSTRACT

The identification of recurrent, protein-altering genetic alterations is frequently the means by which a given gene is initially implicated in tumor biology. Our specific aims are: (1) Carry out the genome-wide identification of nonsynonymous mutations in prostate metastases; (2) Evaluate the mutational histories of individual mutations within the progression of the cancer in which it was observed, and assess prevalence; (3) Perform integrative analyses of somatic mutation with gene expression and copy number change data collected on the same samples. During this funding period we have: (i) completed the identification and quality assessment of the prostate cancer tissues/samples that will be used for the project; (ii) completed DNA isolation for 300 samples/cases of prostate cancer; (iii) Transfered the 1st and 2nd groups of DNAs to the Shendure lab for Exome analysis; (iv) completed exome sequencing on 50 tumor metastasis and completed the analysis of 27 of these exomes; (v) completed CGH assays on 200 prostate cancers; (vi) initiated the integrated analyses of gene expression, copy number and mutation in prostate cancer using network approaches.

15. SUBJECT TERMS
prostate cancer, genomics, exome, sequencing, mutation

16. SECURITY CLASSIFICATION OF:			17. LIMITATION OF ABSTRACT	18. NUMBER OF PAGES	19a. NAME OF RESPONSIBLE PERSON
a. REPORT	b. ABSTRACT	c. THIS PAGE			USAMRMC
U	U	U	UU	30	19b. TELEPHONE NUMBER *(include area code)*

Table of Contents

Introduction (Final Report)

(Unchanged from previous reports): The identification of recurrent, protein-altering genetic alterations is frequently the means by which a given gene is initially implicated in tumor biology. However, we currently lack a comprehensive picture of the protein-altering mutations that are biologically relevant or potentially specific to prostate cancer. The research supported by this award aims to use a new generation of technologies for DNA sequencing to comprehensively scan the genomes of a series of prostate cancers for small mutations that disrupt protein-coding sequences. Our specific aims are as follows: (1) To carry out the genome-wide identification of nonsynonymous mutations in a limited number of prostate metastases using second-generation technologies for targeted capture and sequencing; (2) To evaluate the mutational histories of individual mutations within the progression of the cancer in which it was observed, and to assess the prevalence of candidate cancer genes observed here in prostate cancer. (3) To perform integrative analyses of somatic mutation with gene expression and copy number change data collected on the same samples.

Taking advantage of technological advances in the field, we have expanded the original scope of the project to include a larger number of metastatic samples and a deeper 'discovery' component using whole-exome sequencing approaches followed by assessments of prevalence and function.

Body

This is a "synergy" project between the laboratories of Dr. Jay Shendure in the Department of Genome Sciences at the University of Washington (UW) and Dr. Peter Nelson in the Division of Human Biology at the Fred Hutchinson Cancer Research Center (FHCRC). Because these are separate awards to the two investigators, this progress report is specific to tasks from the statement of work (SOW) assigned to the Nelson Lab only (or to progress within the Nelson Lab for joint tasks). As per the instructions, progress is reported in association with each of the relevant tasks listed in the SOW. Each of the following Tasks has been updated, where appropriate, with new data and information since the Year 2 progress report and now is inclusive of Year 1-3.

Aim 1: Perform a comprehensive screen for protein coding alterations in prostate metastases.

Task 1. Select tumors to be subjected to exome sequencing (Months 1-2) **[FHCRC]**

In Years 1-2 of this project, we obtained 300 prostate cancer specimens. These included 60 primary prostate cancers, 24 prostate cancer xenografts primarily representing advanced prostate cancer, and 216 metastatic prostate cancers. In the majority of cases, the metastatic prostate cancers represent multiple metastasis (≥2 each) from each of 54 patients. Each tumor sample was embedded in OCT, sectioned, and evaluated for percentage of tumor by hematoxylin and eosin staining and pathological review. *Task Complete*.

Task 2. Tumor tissue processing and quality control (Months 2-3) **[FHCRC]**

From each tumor specimen, sections were cut on a cryostat and RNA and DNA was extracted (Qiagen micro RNA and DNA purification columns/reagents). The quantity of RNA and DNA was determined by NanoDrop methods. The quality of RNA and DNA was determined by Agilent Bioanalyzer assays. In total, 10 samples did not pass q/c assessments for a total success rate of 96%. DNA for exome capture and sequencing studies was transferred to the Shendure Lab. *Task Complete*.

Task 3. DNA isolation and shotgun library construction (Months 4-10) [UW]

Performed in Shendure lab—see companion Progress Report.

Task 4. Array-based enrichment of coding sequences (Months 7-13) [UW]

Performed in Shendure lab—see companion Progress Report.

Task 5. Massively parallel sequencing of tumor and control exomes (Months 10-16) [UW]

Performed in Shendure lab—see companion Progress Report.

Task 6. Read mapping, variant calling, and mutation annotation (Months 11-17) [UW]

Performed in Shendure lab—see companion Progress Report.

Aim 2: Evaluate mutational histories and prevalence screen of candidate cancer genes.

Task 7. Design & testing of MIP-based capture assay. (Month 18-20) **[FHCRC]**

Work on this Task has commenced and the original Task is completed. However, based on technological advances (and attendant lower assay costs), we have expanded the task to include additional variants. This task is based on the identification of novel non-synonymous nucleotide variants (nov-SNVs) identified from the first 24 exome sequences and additional assessments of 20 tumor exomes analyzed through the Nelson/Shendure studies, and recent collaborative work conducted with the Rubin/Garraway group (see reportable outcome publication Barbieri et al 2012 *Nature Genetics*). These nov-SNVs are detailed in the Progress Report from the Shendure lab, and include: p53 mutations, SPOP mutations, MSH6, SPOP mutations and others. Note, although originally assigned as a task to the Nelson lab, the MIP-based capture assay is performed in the Shendure lab. *Task Complete*.

Task 8. Selection and q/c of validation tissues (Month 8-16) **[FHCRC]**

We have identified a cohort of 300 primary prostate cancers with attendant formalin fixed paraffin-embedded tissues from the pathology archives at the University of Washington. Each of these cases was selected based on outcomes data of relapse versus non-relapse following radical prostatectomy. For these 300 of these cases, we have completed a pathology review to identify cancer and benign prostate regions, and obtained a 'punch' of these corresponding tissues that will be used for DNA preparations. For an additional 60 prostate cancer cases, comprised primarily of metastasis, we have verified the histology, and completed the isolation of DNA (see Task 9). *Task Complete*.

Task 9. Preparation of DNA for validation tissues (Month 9-18) **[FHCRC]**

For 300 prostate cancer cases we have completed DNA extraction. Q/C of A260/280 ratios was performed and all samples passed this analysis. The preparations of DNA from the 300 primary

prostate cancers with outcomes is now complete. Q/C overall has confirmed that 80% of cases are of suitable quality for subsequent assays. *Task Complete*.

Task 10. Application to evaluate mutation histories (Months 20-24) [UW]

This task was performed primarily in the Shendure lab (see Progress Report from the Shendure Lab). However, to perform initial verification/validation studies, we evaluated the mutation calls for several genes discovered initially by the Exome capture and NextGen sequencing (see Shendure Progress Report). We confirmed the exome calls for mutations in the *speckle-type POZ protein* (SPOP) gene, involved in mediating SRC-3/AIB1 activity—and consequently the activity of the androgen receptor, and determined that these genes are recurrently mutated in prostate cancers. The preliminary data for this finding was shown in the Year 1 and Year 2 progress reports. Below is a figure from our collaborative study with the Rubin/Garraway group demonstrating the recurrent alterations of SPOP across multiple prostate cancer datasets including data generated in the context of this research project (Figure 1).

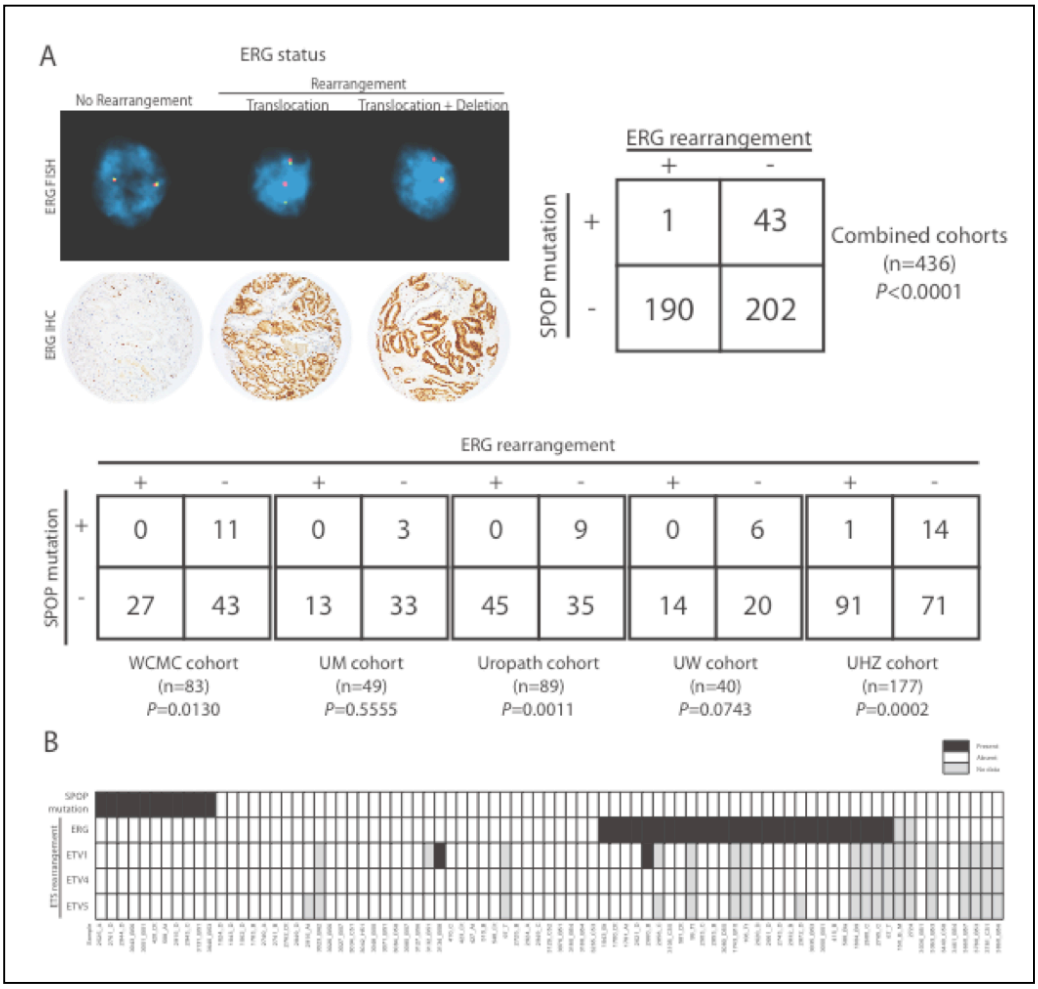

***Figure 1.* SPOP mutations are recurrent across different prostate cancer cohorts and are mutually exclusive with respect to ERG rearrangements. Data from this research project are shown under the 'UW cohort'.**

We completed an assessment of common/recurrent non-synonymous mutations in metastatic prostate cancers identifying several new genes with high frequency mutations that include ADAM21, FAT3, IGSF3, and DSPP (Figure 2). Further studies are required to determine the phenotypic consequences of these mutations. *Task Complete*.

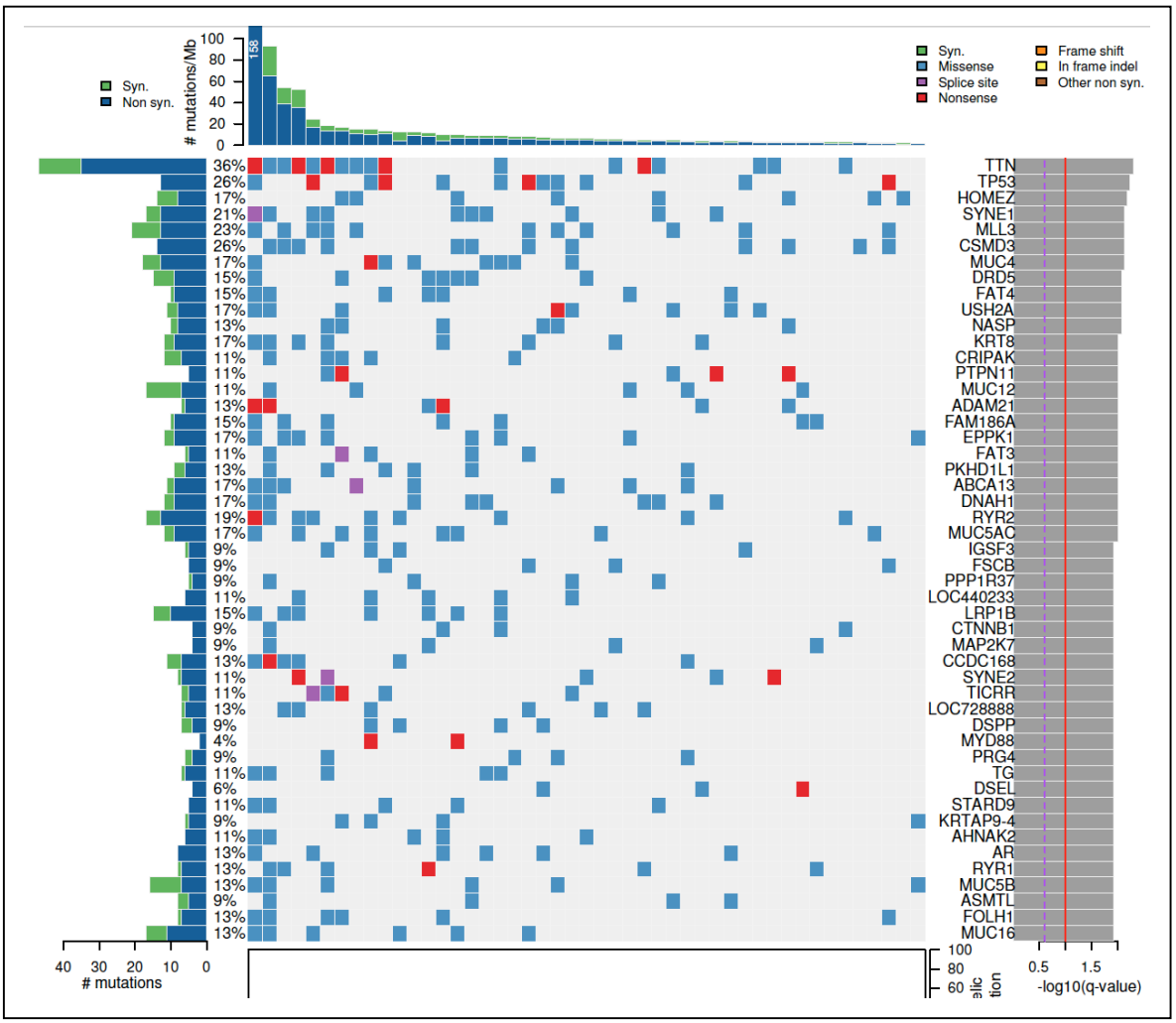

Figure 2. Plot of the frequency of non-synonymous mutations identified in prostate cancer metastasis. A representative tumor from each of 54 patients is depicted. Color coding denotes the type of mutation (e.g. missense vs nonsense).

Task 11. Application to prevalence screen of candidate cancer genes (Months 18-30) [UW]

See Shendure lab progress report.

Task 12. Read mapping, variant calling, and mutation annotation (Months 21-31) [UW]

See Shendure lab progress report.

Task 13. Verification/confirmation of sequence variants (Months 20-26) [UW]

See Shendure lab progress report.

Aim 3: Integrate analyses of molecular alterations in metastatic and primary prostate cancer.

Task 14. Development of algorithms for integrative analysis (Months 1-12) **[FHCRC]**

In collaboration with Dr. Pei Wang, and the SAGE bioinformatics group (Dr. Brig Mecham and Dr. Jonathan Derry) located at FHCRC (http://sagebase.org/), we have developed approaches to homogenize disparate datasets provide complementary information regarding signaling pathways operating in prostate cancers. These take advantage of network-based analyses using coherent datasets (e.g. data from the same sample) involving transcript profiles, copy number variation, and nucleotide sequence (e.g. mutation) analyses. We assessed the output of these algorithms for defining key activity nodes that can be modulated for therapeutic targeting and for understanding drivers of prostate cancer development and progression. Figure 3 depicts a network map based on transcript profiles and copy number alterations in prostate cancer that center on the ERG oncogene. Algorithms complete. *Task Complete.*

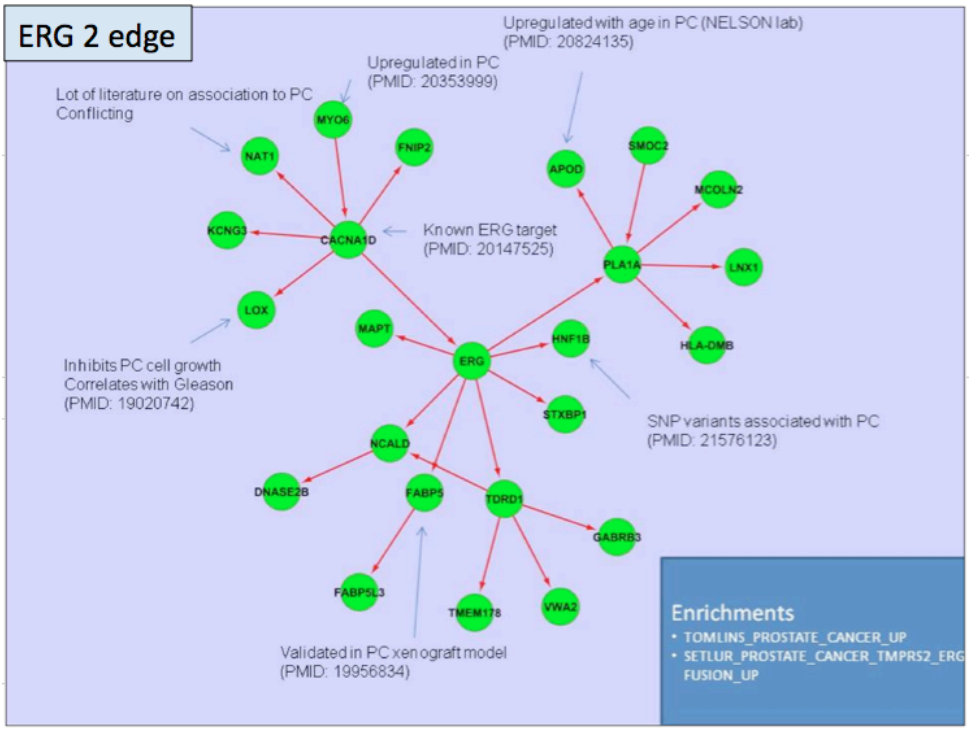

Figure 3. Network map of the ERG node defined by copy number and gene expression changes in prostate cancer metastasis. Known ERG-relationships were identified (CACNA1D). Several novel predicted interactions were also identified that include the cell stress mediator APOD.

We have utilized the integrated analysis algorithms to assess the intra-patient patient

We have utilized the integrated analysis algorithms to assess the intra-patient variation in molecular alterations in order to assess the divergence or consistency of alterations that may occur in different metastasis from the same patient. The practical use of this information concerns the concepts of tumor sampling for precision medicine. The key question concerns whether sampling a single metastasis represents the relevant molecular changes in other metastasis. An example of this analysis is shown in Figure 4 where nine metastasis and a primary tumor from the same patient are compared using mutation analysis, copy number analysis, and gene expression. The vast majority of the changes found in the primary tumor are also found in each of the metastasis, and concordantly, the vast majority of changes found in any particular

metastasis are also found in other metastasis. However, there are notable exceptions where certain metastasis appear to have diverged and both gained and lost alterations found in other tumors from the same individual. *Task Complete.*

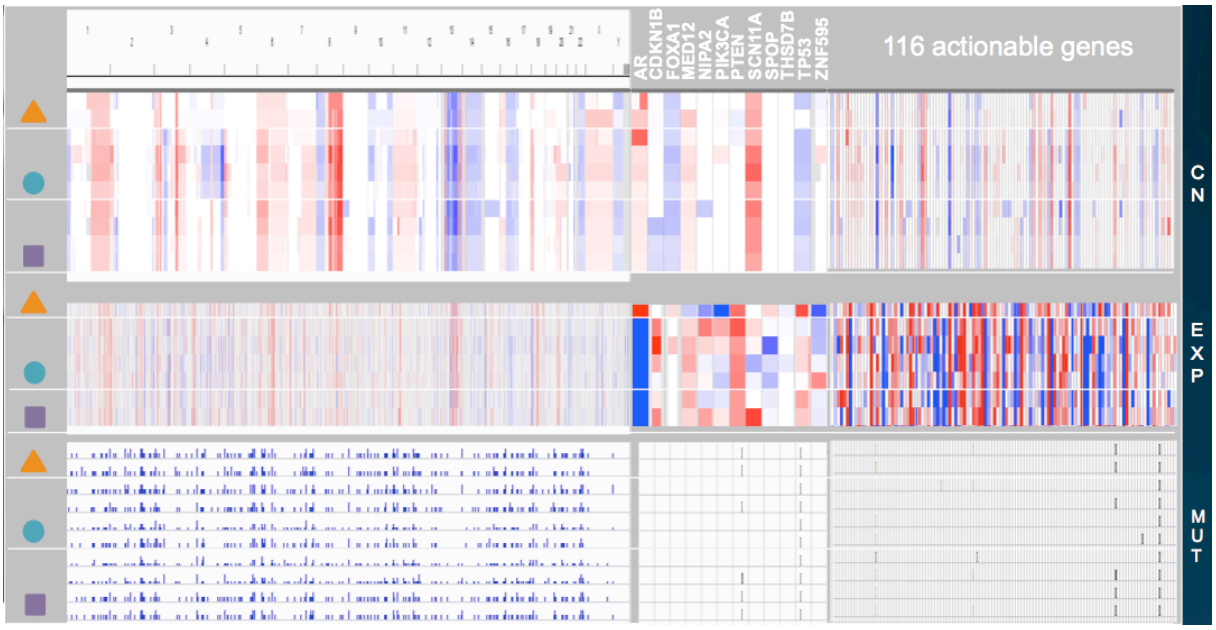

Figure 4. Integrated analysis of DNA copy number (CN-top), gene expression (EXP-middle) and mutation (MUT-bottom) across 9 tumors from the same patient. To the left in circle, square and triangle are groups of tumors with the most highly concordant constellation of molecular changes. In this patient, the vast majority of alterations are conserved across all 9 tumors and thus sampling a single tumor would provide a good assessment of the changes occurring in other metastasis.

Task 15. Analysis of mutational patterns in metastatic prostate cancer (Months 11-17) [UW]

The studies of SPOP mutations included a spectrum of metastatic prostate cancers demonstrating an overall mutation frequency of ~12%. An interesting result is the identification of a mutation in the BRAF oncogene. A molecular analysis using Molecular Inversion Probe (MIP) sequencing revealed a mutation at position 601 in the BRAF gene, leading to a lysine-to-glutamate substitution. This mutation was subsequently confirmed using Sanger sequencing in the index metastasis as well as seven other metastases from the same patient. See Shendure Lab progress report.

Task 16. Analysis of mutational patterns in primary prostate cancer (Months 21-31) [UW]

The studies of SPOP mutations included a spectrum of primary prostate cancers demonstrating an overall mutation frequency of ~12%. See Shendure lab progress report. We have integrated the analysis of mutations that occur with high frequency in metastasis with their frequency in primary prostate cancers. This analysis provided a number of mutations that appear to only occur in advanced castration-resistant prostate cancer, suggesting roles in the metastatic process and/or emerging to drive treatment resistance (Figure 5). These studies lay the groundwork for

subsequent mechanistic assessments of the phenotypic consequences of these mutations. *Task Complete.*

GENE	UW	UM	Garraway	EurUrol	Other	t-test p value		AA Size
ZNF646	6.7%	6.5%	0.0%	1.6%	0.0%	0.01	TRUE	1833
CSMD1	6.7%	8.1%	1.8%	0.0%	1.7%	0.01	TRUE	3565
ABCA13	11.1%	11.3%	4.4%	0.0%	2.3%	0.02	TRUE	5059
AR	8.9%	8.1%	0.0%	0.0%	0.0%	0.03	TRUE	921
CNTNAP5	6.7%	4.8%	0.0%	0.0%	2.3%	0.04	TRUE	1307
PLEC	4.4%	6.5%	2.7%	0.0%	0.6%	0.07	TRUE	4575
NEB	4.4%	6.5%	2.7%	0.0%	1.1%	0.07	TRUE	8526
MLL2	6.7%	4.8%	0.9%	0.0%	1.1%	0.08	TRUE	5538
CNTNAP2	6.7%	4.8%	0.9%	0.0%	0.0%	0.08	TRUE	1332
RYR1	8.9%	6.5%	1.8%	3.1%	1.1%	0.09	TRUE	5039
VCAN	6.7%	4.8%	3.5%	3.1%	0.6%	0.09	TRUE	2410
ZFHX3	8.9%	6.5%	0.9%	0.0%	0.6%	0.09	TRUE	2790
RYR3	6.7%	9.7%	1.8%	0.0%	1.7%	0.10	TRUE	4871
TRPA1	4.4%	6.5%	0.9%	0.0%	0.0%	0.10	TRUE	1120
CDC42EP1	4.4%	6.5%	0.9%	0.0%	0.0%	0.10	TRUE	392
FSIP2	6.7%	4.8%	0.0%	0.0%	0.0%	0.10	TRUE	6997
DGKB	4.4%	6.5%	0.0%	0.0%	0.0%	0.12	TRUE	805
MUC16	8.9%	8.1%	3.5%	0.0%	6.9%	0.12	TRUE	14508
TP53	20.0%	29.0%	5.3%	10.9%	6.3%	0.13	TRUE	394
USH2A	13.3%	8.1%	1.8%	1.6%	1.7%	0.18	TRUE	5203
ZFHX4	8.9%	4.8%	2.7%	0.0%	1.1%	0.19	TRUE	3617
CTNNB1	8.9%	4.8%	0.0%	1.6%	2.9%	0.19	TRUE	782
FAT4	13.3%	6.5%	5.3%	0.0%	1.7%	0.23	TRUE	4982
PKHD1L1	11.1%	4.8%	0.0%	0.0%	1.7%	0.25	TRUE	4244
DNAH11	2.2%	8.1%	0.0%	0.0%	0.0%	0.33	TRUE	4524
TG	8.9%	3.2%	0.9%	3.1%	0.6%	0.34	TRUE	2769
OBSCN	8.9%	3.2%	2.7%	0.0%	2.3%	0.35	TRUE	7969
RYR2	11.1%	3.2%	1.8%	0.0%	4.0%	0.40	TRUE	4968
TTN	24.4%	6.5%	8.0%	1.6%	15.4%	0.57	TRUE	34351
MLL3	15.6%	1.6%	0.9%	7.8%	1.7%	0.59	TRUE	4912
MUC4	15.6%	3.2%	0.9%	1.6%	12.0%	0.60	TRUE	5413
SYNE1	15.6%	1.6%	3.5%	4.7%	3.4%	0.62	TRUE	8750
USP28	4.4%	4.8%	0.9%	1.6%	0.0%	0.01	FALSE	1078
PIK3C2A	4.4%	4.8%	0.0%	1.6%	0.0%	0.01	FALSE	1687
SPOP	4.4%	3.2%	12.4%	9.4%	8.0%	0.03	FALSE	375

Figure 5. A comparative assessment of non-synonymous mutations in metastatic prostate cancer versus primary untreated prostate cancers. The frequencies determined from our studies are shown in the orange 'UW' column representing 54 patients. The orange column UM study contributes another 50 metastatic patients. The three blue columns represent ~200 primary prostate cancers from three studies. The t-test value comparies the significance of mutations in metastatic prostate cancer vs primary. The androgen receptor (AR) represents an example of a gene that is never mutated in primary prostate cancer but is frequently mutated in advanced CRPC. SPOP represent a gene that is mutated at the same frequency in primary and metastatic prostate cancer, suggested it is an early driver mutation.

Task 17. Analysis of copy number alterations in prostate cancer (Months 6-31) **[FHCRC]**

We have now completed the analysis of copy number variation (CNV) across 200 prostate cancers (using DNA extracted from samples in Aim 1, a subset of which have also been used for mutation analyses by exome sequencing). We have identified several genomic regions with recurrent alterations including regions in 8p, 8q, PTEN, RB, NCOA2, and AR. Data demonstrating regions with frequent loss were shown in the Year 1 progress report. No new regions of high copy number loss/gain have been identified (Figure 6). *Task Complete*.

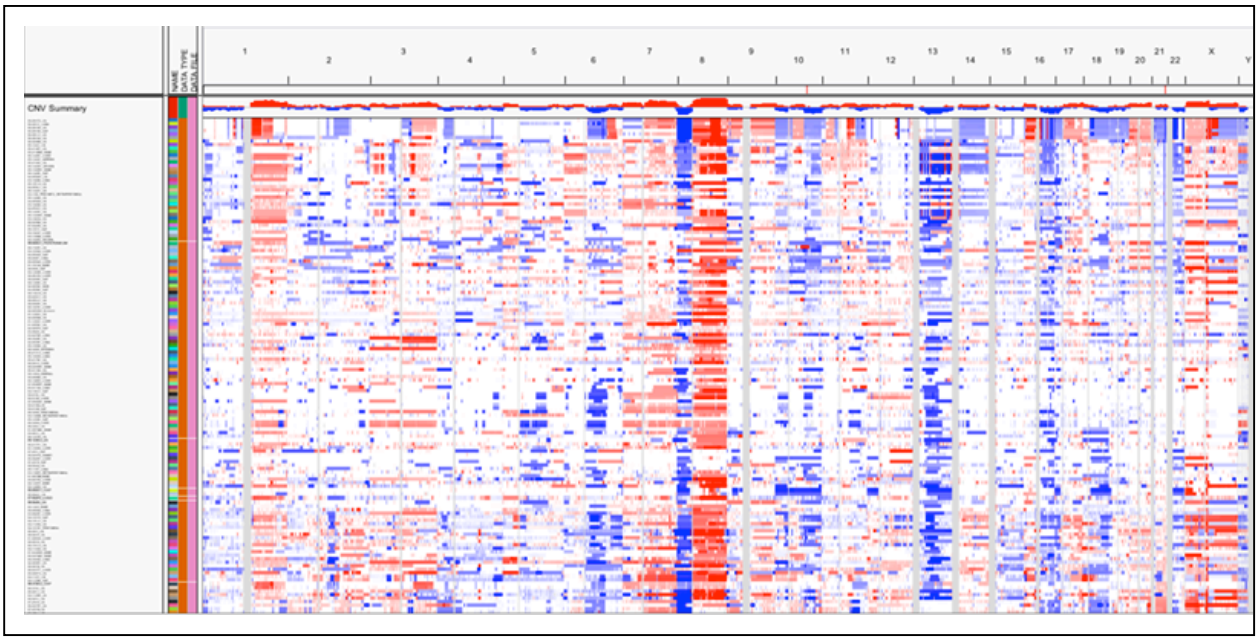

Figure 6. Array CGH-based assessment of DNA copy number across prostate cancer metastasis. Note high frequency gains (red) and losses (blue) in 8p, 8q, Chromosome 10 (Pten loss), and X chromosome (AR).

Task 18. Analysis of consequences of genome alterations (protein/mRNA) (Months 18-28) [FHCRC]

We have determining associations between somatic copy number variation and transcript levels, both in the context of cis-acting and trans-acting effects (Figure 7-9). We have also analyzed the consequences of copy number alterations in key prostate cancer genes: TMPRSS2-ERG, PTEN, and AR. We found that aberrations in these genes was significantly more common in metastatic prostate cancers compared to primary tumors, and that mRNA levels associated with genomic copy loss or gain (see reportable outcomes (Qu, X et al). *Task Complete.*

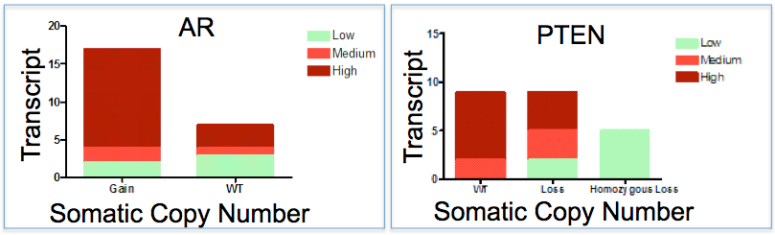

Figure 7 Association between copy number and mRNAs for AR (left) and PTEN (right) across a series of prostate cancer metastasis.

Cis-acting eCNVs

For a given gene, we measured correlations between its RNA expression and each of the CNVs corresponding to that gene. The maximal correlation was taken for each gene and we defined a cis-acting CNV as any where the correlation was greater than 0.6. Here are these 104 genes:

ADK	ATAD1	CMAS	EBAG9	GPBP1	IPO8	MBTPS1	MYST4	PPP3CC	RIPK2	SYNCRIP	TRAM1	WHSC1L1
AGPAT6	ATAD2	COPS5	EIF2C2	GSTM1	KIAA0174	MCPH1	NCOA2	PRKDC	RNF170	TAF2	TXNL4B	WRN
ANKRD46	ATP6V1C1	CPNE3	ELP3	GSTT1	KIAA0196	MIER3	NUDCD1	PSMD7	RRM2B	TCEB1	UBE2W	WWP1
AP1G1	ATP6V1H	CSPP1	FAM49B	HLA-DRB5	KIAA0528	MRPS28	ORM1	PTDSS1	RSPRY1	TERF1	VAC14	XPO7
AP3M2	C18orf25	CYB5B	FAM82B	HOOK3	KIAA0564	MTDH	OTUD6B	PTEN	SLC20A2	TERF2	VDAC3	YWHAZ
AR	C8orf40	DECR1	FNDC3A	HPR	KIAA1429	MTERFD1	PCM1	PTK2	SPAG1	TMEM30A	VPS13B	ZC3H13
ARFGEF1	CDC40	DYM	GHITM	IMPA1	LACTB2	MTUS1	PDPR	RAD21	STAU2	TMEM68	VPS37A	ZFAND1
ARMC1	CHMP4C	DYNC1LI2	GOLGA7	INTS8	MAP3K7	MYST3	PHF20L1	RB1CC1	SUCLA2	TNKS	WDR59	ZNF706

Figure 8 Table of CNVs that have significant associations with transcript levels across primary and metastatic prostate cancers.

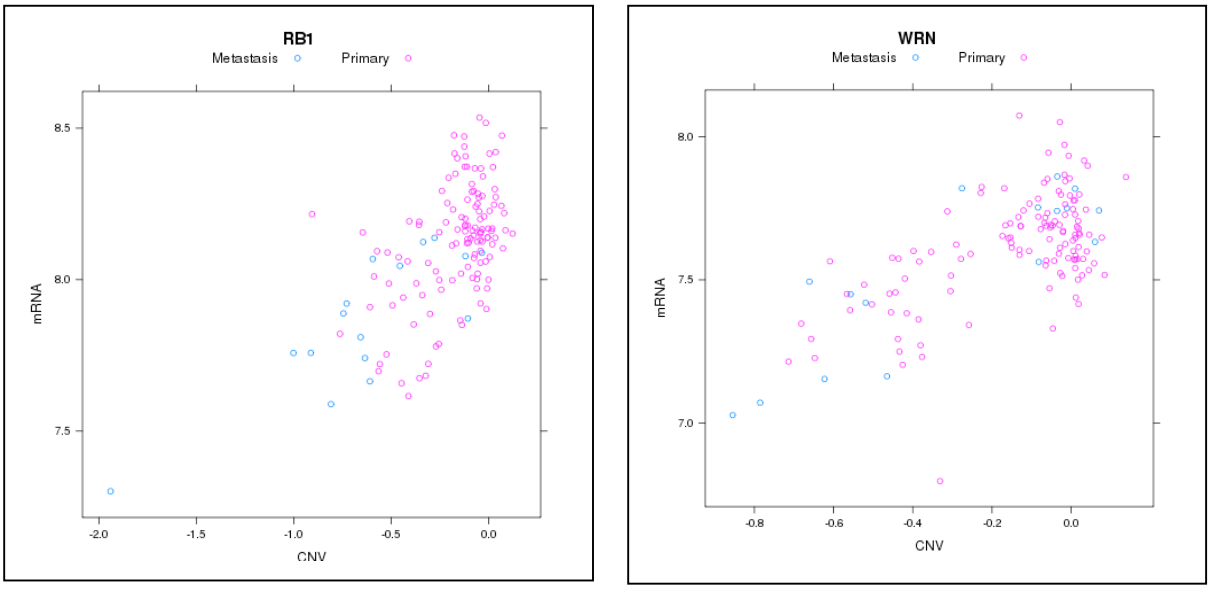

Figure 9. Example of an expected (RB1) and novel (WRN) cis-regulatory association between somatic gene copy number and mRNA. RB1 loss has been previously demonstrated to occur frequently in metastatic prostate cancer and associates with loss of RB1 expression. The WRN gene is involved in DNA repair and has not previously been shown to be associated with prostate cancer.

Task 19. Integrative pathway analysis of DNA alterations. (Months 8-34) **[FHCRC]**

We have completed the integration of coherent prostate cancer data as described and depicted under Task 14 above. The data in Figure 10 and Figure 11 depict the integration of common mutation status and copy number variation across the prostate cancer metastasis. As previously noted, the majority of alterations are consistent across metastasis from the same patients, though there are notable outliers where a specific tumor may diverge from others in the same patient. *Task Complete.*

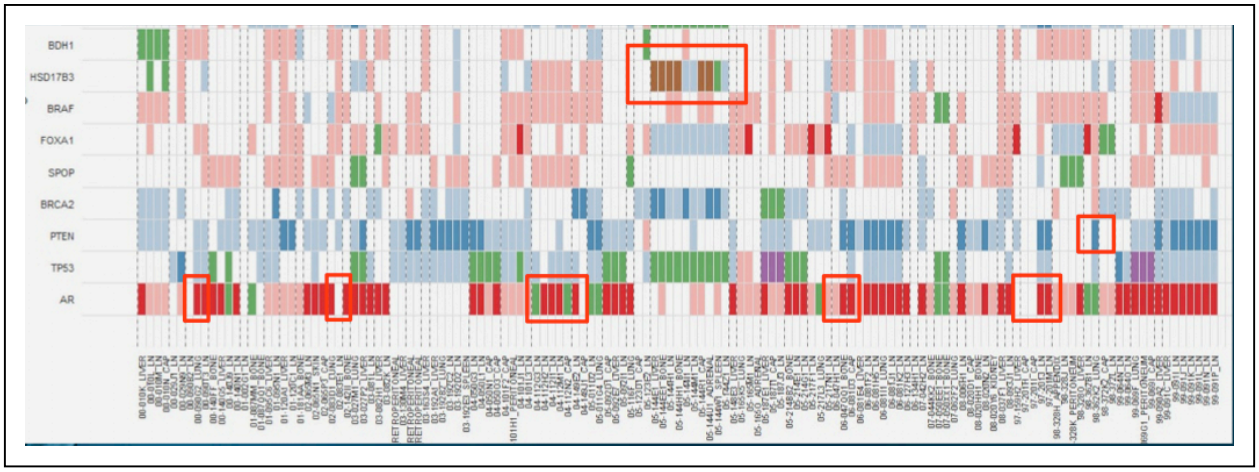

Figure 10 and 11. Integrated analysis of mutation and copy number alterations in prostate cancer metastasis. Consistent alterations across patients with one representative tumor per patient (Figure 10, Top). Intrapatient variability is highlighted (Figure 11, Bottom) with red boxes emphasizing variation in multiple tumors from the same individual.

Task 20. Integrative analysis for expression and DNA alterations (Month 18-34) **[FHCRC]**

We have completed RNA preparations and expression profiling by microarray analysis for 150 prostate cancers. The remaining integrated analyses are underway. We have integrated with expression profiling data with other tumor characteristics and with the molecular assessments of copy number and with mutation status.

One notable result of these analyses center on defining a mechanism for a sub-class of prostate cancers that exhibit a 'hyper-mutation' phenotype. We have found that approximately 8-10% of prostate cancers are hypermutated with ~10-fold more mutations than are normally found. We have found that these tumors exhibit a classic microsatellite instability (MSI) phenotype and express far less MSH2 or MSH6 transcript and protein levels. Through detailed genomic assessments of these hypermutated tumors, we have determined that the MSH2 or MSH6 loss is due to a chromosomal alteration comprising gene translocation or deletion (Figure 12). Future studies will determine whether these hypermutated tumors exhibit differential responses to specific treatments as an 'actionable' subtype of prostate cancer. *Task Complete*.

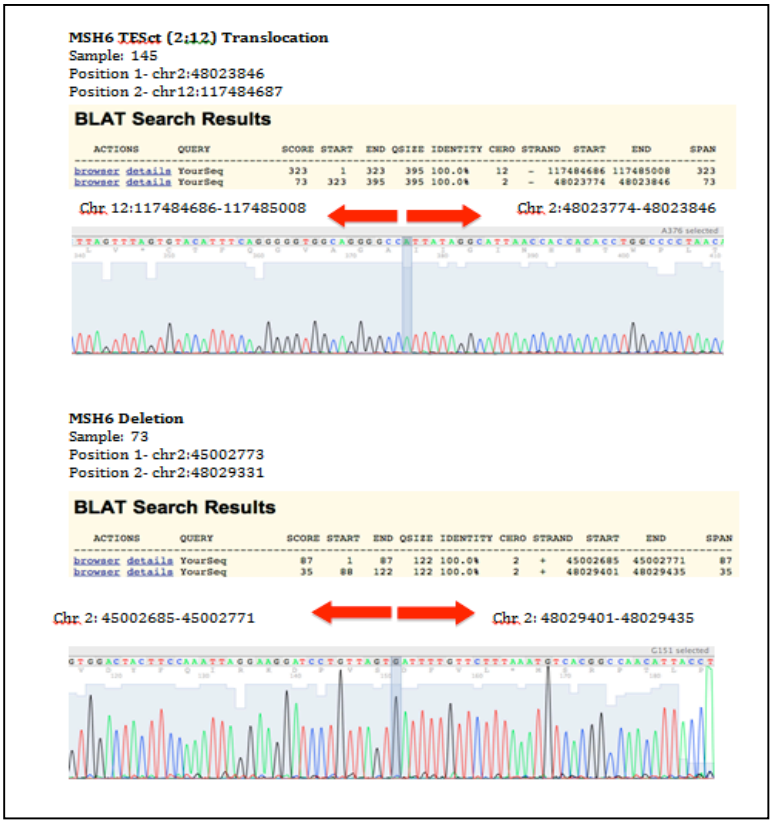

Figure 12. Identification of the underlying cause of hyper-mutated prostate cancers. Genomic alterations in mis-match repair genes was identified in the hypermutated subtype of prostate cancer. Detailed genomic sequencing analyses identified translocations or deletions in key mismatch repair genes. Shown are two cases where MSH6 is disrupted: translocation (top) and deletion (bottom).

Task 21. Annotating and posting project data to website (Months 18-36) **[UW & FHCRC]**

We have opted to post and present all project data onto a widely used publicly available website, cBio, hosted at Memorial Sloan Kettering Cancer Center. This website hosts cancer genome data from a wide variety of sources, and thus having this prostate cancer metastasis data together with other data will facilitate the use of the data by other investigators by allowing them to visit one site for access. Further, the cBio site has a suite of analysis tools that are continuing being

updated and improved to allow investigators to query the data and perform analyses to test their hypotheses and genes of interest. We have uploaded all project data to the cBio site where it is currently being curated for public presentation. *Task Complete.*

Task 22. Completing project reports and manuscripts (Months 11-36) **[UW & FHCRC]**

This report represents the final project progress report. In addition, two manuscripts are in preparation that will provide a detailed analysis of the integrated project data. Manuscript 1 focuses on the full analysis of intra- and inter-individual molecular alterations that occur in advanced metastatic prostate cancer. The second manuscript focuses on the molecular mechanism underlying the MSI hypermutated tumors. An abstract detailing this study was presented at the Prostate Cancer Foundation meeting 10/2013 and is included in the reportable outcomes. *Task: Report Complete and additional manuscripts are in progress.*

Key Research Accomplishments

- We have completed the identification and quality assessment of the prostate cancer tissues/samples that were used for the duration of the project.
- We completed DNA isolation for 300 samples/cases of prostate cancer used for the project experiments.
- We have sequencing 150 prostate cancer exomes from multiple tumors derived from 54 patients.
- We have interpreting the Exome sequence data for the 150 primary prostate cancers and metastasis. These studies have produced the exciting and novel result identifying a 'hypermutated' prostate cancer phenotype. (see Reportable Outcomes: Kumar et al[1]).
- In collaboration with the Shendure lab we have identified, and confirmed, recurrent point mutations in several genes and genetic pathways. These include recurrent mutations in p53 and in the ubiquitin ligase component SPOP (see Reportable Outcomes: Barieri et al[2]).
- We have completed array CGH analyses of copy number variation across 150 prostate cancers. We have confirmed these alterations by additional methods such as fluorescence in situ hybridization and determined that the copy number changes in key genes such as AR and Pten occur are significantly greater frequency in advanced relative to localized prostate cancers (see Reportable Outcomes Qu et al[4])
- We have completed network-based integrated molecular analyses of advanced prostate cancers that include copy-number variation and transcript profiles.
- We have found a novel mechanism which underlies the hypermutated phenotype of prostate cancer involving the genomic disruption of key mismatch repair genes MSH2/MSH6 (see Reportable Outcomes: Pritchard et al[3]). A manuscript is in preparation detailing these results.
- We have uploaded all molecular data (transcript profiles, mutation calls, copy number changes) to the cBio portal for cancer genomics (www.cbioportal.org/public-portal/) for data dissemination to the community.

Reportable Outcomes

1. Kumar, A. *et al.* Exome sequencing identifies a spectrum of mutation frequencies in advanced and lethal prostate cancers. *Proc Natl Acad Sci U S A* 108, 17087-92 (2011). PMCID: 3193229

2. Barbieri, C.E. *et al.* Exome sequencing identifies recurrent SPOP, FOXA1 and MED12 mutations in prostate cancer. *Nat Genet* 44, 685-9 (2012).

3. Colin C. Pritchard, Colm Morrissey, Akash Kumar, Xiaotun Zhang, Christina Smith, Ilsa Coleman, Stephen Salipante, Jonathan F. Tait, Robert Vessella, Tom Walsh, Jay Shendure, and Peter S. Nelson *(2013) MSH2* and *MSH6* Structural Rearrangements in Hypermutated Microsatellite Unstable Advanced Prostate Cancer. *Prostate Cancer Foundation Annual Meeting*.

4. Qu X, Randhawa G, Friedman C, Kurland BF, Glaskova L, Coleman I, Mostaghel E, Higano CS, Porter C, Vessella R, Nelson PS, Fang M. (2013) A Three-Marker FISH Panel Detects More Genetic Aberrations of AR, PTEN and TMPRSS2/ERG in Castration-Resistant or Metastatic Prostate Cancers than in Primary Prostate Tumors. *PLoS One*. Sep 30;8(9):e7467

Conclusion

In summary, by characterizing the genomes (mutation analysis; copy number variation; gene expression) of prostate tumors representing a spectrum of aggressive advanced prostate cancers, we have identified: (1) previously unrecognized gene coding variants with the potential to influence tumor behavior; (2) common and rare structural variations in prostate cancer genomes; (3) a previously unrecognized subtype of 'hypermutated' prostate cancer; (4) a genetic mechanism that underlies the hypermutated prostate cancer subtype; (5) relationships between mutation and copy number variation and the cis- and trans-activating effects of these aberrations in gene and protein expression; (6) intra-patient consistency and intra-patient variability in genomic aberrations across metastasis. This finding serves as an reference for the accuracy of precision medicine approaches that sample individual tumors that potentially reflect aberrations in unsampled tumors. Finally, the data from this study have been provided to a publicly accessed database (cBio) for the rapid and widespread dissemination of molecular data derived from metastatic castration resistant prostate cancer, a disease entity that has heretofore been quite difficult to derive detailed molecular information that could guide new treatment strategies.

OPEN ACCESS Freely available online

PLOS ONE

A Three-Marker FISH Panel Detects More Genetic Aberrations of *AR*, *PTEN* and *TMPRSS2/ERG* in Castration-Resistant or Metastatic Prostate Cancers than in Primary Prostate Tumors

Xiaoyu Qu[1], Grace Randhawa[2], Cynthia Friedman[2], Brenda F. Kurland[1], Lena Glaskova[2], Ilsa Coleman[1], Elahe Mostaghel[1,3], Celestia S. Higano[1,2,3], Christopher Porter[4], Robert Vessella[3,5], Peter S. Nelson[1,3], Min Fang[1,2,3]*

1 Fred Hutchinson Cancer Research Center, Seattle, Washington, United States of America, **2** Seattle Cancer Care Alliance, Seattle, Washington, United States of America, **3** University of Washington, Seattle, Washington, United States of America, **4** Virginia Mason Medical Center, Seattle, Washington, United States of America, **5** Puget Sound VA Health Care System, Seattle, Washington, United States of America

Abstract

TMPRSS2/ERG rearrangement, *PTEN* gene deletion, and androgen receptor (*AR*) gene amplification have been observed in various stages of human prostate cancer. We hypothesized that using these markers as a combined panel would allow better differentiation between low-risk and high-risk prostate cancer. We analyzed 110 primary prostate cancer samples, 70 metastatic tumor samples from 11 patients, and 27 xenograft tissues derived from 22 advanced prostate cancer patients using fluorescence in situ hybridization (FISH) analysis with probes targeting the *TMPRSS2/ERG*, *PTEN*, and *AR* gene loci. Heterogeneity of the aberrations detected was evaluated. Genetic patterns were also correlated with transcript levels. Among samples with complete data available, the three-marker FISH panel detected chromosomal abnormalities in 53% of primary prostate cancers and 87% of metastatic (Met) or castration-resistant (CRPC) tumors. The number of markers with abnormal FISH result had a different distribution between the two groups ($P<0.001$). At the patient level, Met/CRPC tumors are 4.5 times more likely to show abnormalities than primary cancer patients ($P<0.05$). Heterogeneity among Met/CRPC tumors is mostly inter-patient. Intra-patient heterogeneity is primarily due to differences between the primary prostate tumor and the metastases while multiple metastatic sites show consistent abnormalities. Intra-tumor variability is most prominent with the *AR* copy number in primary tumors. *AR* copy number correlated well with the *AR* mRNA expression (rho = 0.52, $P<0.001$). Especially among *TMPRSS2:ERG* fusion-positive CRPC tumors, *AR* mRNA and *ERG* mRNA levels are strongly correlated (rho = 0.64, $P<0.001$). Overall, the three-marker FISH panel may represent a useful tool for risk stratification of prostate cancer patients.

Citation: Qu X, Randhawa G, Friedman C, Kurland BF, Glaskova L, et al. (2013) A Three-Marker FISH Panel Detects More Genetic Aberrations of *AR*, *PTEN* and *TMPRSS2/ERG* in Castration-Resistant or Metastatic Prostate Cancers than in Primary Prostate Tumors. PLoS ONE 8(9): e74671. doi:10.1371/journal.pone.0074671

Editor: Dean G. Tang, The University of Texas M.D Anderson Cancer Center, United States of America

Received May 3, 2013; **Accepted** August 4, 2013; **Published** September 30, 2013

Funding: This study was supported by PNW SPORE P50 CA097186, P50CA138293, P01CA085859, PC093372, and PC093509 awarded by the National Cancer Institute. The xenograft generation and clinical specimen collection was supported by Richard M. Lucas Foundation. The funders had no role in study design, data collection and analysis, decision to publish, or preparation of the manuscript.

Competing Interests: The authors have declared that no competing interests exist.

* E-mail: mfang@fhcrc.org

Introduction

The discovery of recurrent *ETS* gene rearrangements in prostate cancers has led to studies evaluating the functional role of *ETS* genes in the pathogenesis of this disease and as diagnostic and prognostic biomarkers. The most common type of *ETS* rearrangement, the fusion of androgen-regulated *TMPRSS2* with the oncogenic *ERG* is detected in approximately half of prostate tumors but none of benign glands [1]. However, studies assessing the prognostic significance of *TMPRSS2:ERG* fusion have yielded inconsistent results [2–5]. Additional genetic factors are likely to work in concert with the fusion during cancer progression. Recent studies have shown that genetic aberrations are not only common in prostate cancer but also interact with each other through related pathways, thereby contributing to the progression to invasive diseases. *TMPRSS2* is regulated by androgens, and the androgen receptor (AR) is often amplified in patients treated with androgen deprivation therapy [6,7]. *PTEN* deletion, another common aberration in prostate cancer, was correlated with the expression of downstream p-Akt and associated with cancer-specific mortality [8,9]. *ETS* gene rearrangements were shown to cooperate with *PTEN* deletion and impact prostate cancer prognosis [10,11]. Crosstalk between PI3K and AR signaling pathways was recently suggested as a mechanism for the development of castration resistant prostate cancer (CRPC) [12,13]. *PTEN* deletion was shown to suppress androgen-responsive gene expression by modulating *AR* transcription factor activity. Also, *PTEN* and *AR* expression has been shown to inversely correlate in prostate cancer [14].

A critical clinical question concerns identifying characteristics of newly diagnosed prostate cancers that will distinguish aggressive from indolent behavior. The molecular heterogeneity of prostate cancers suggests that individual biomarkers may not be sufficient, and that multiple genetic markers may better associate with outcome. In the present study, we used a three-marker fluorescence in situ hybridization (FISH) panel to detect *TMPRSS2* and/or *ERG* rearrangements, *AR* gene amplification, and *PTEN* deletion in both primary and CRPC prostate cancer samples and compared the prevalence, concurrence, and interaction of these three markers. With the reference of mRNA expression data generated from matching tumor samples from the same patient, we also demonstrated how FISH findings correlated with changes in gene expression. Intra- and inter-patient tumor heterogeneity was also analyzed.

Materials and Methods

Sample Acquisition

Ethics Statement. The study was approved by the Institutional Review Boards (IRB) of the Fred Hutchinson Cancer Research Center and the University of Washington Medical Center. IRB waived the need for written consent for this study because only de-identified materials were used, which were from the University of Washington Urology tissue bank.

Patient samples. De-identified archived untreated primary prostate cancer samples (n = 110) were obtained from the University of Washington (UW) and Virginia Mason Hospital in Seattle. A total of 83 primary tumors generated analyzable data for at least one FISH marker in the panel, including 69 patients with *TMPRSS2/ERG* FISH data, 65 patients with *AR* FISH data and 42 patients with *PTEN* FISH data. Metastatic tumor samples (n = 70) were collected at UW from autopsies performed within 2 to 4 hours of death of 11 CRPC patients under the rapid autopsy program [15]. Tumors were obtained from various organ sites, frozen immediately and stored at −80°C. All tissues were sectioned for H&E staining and, for verification of histology, reviewed by a pathologist. FISH analysis was focused on cancer areas. A total of 67 tumors yielded analyzable data for at least one FISH marker in the panel, including 56 tumors from 10 patients with *TMPRSS2/ERG* FISH data, 65 tumors from 11 patients with *AR* FISH data, and 62 tumors from 11 patients with *PTEN* FISH data.

Prostate cancer xenografts. Prostate cancer xenografts (LuCaP lines) were originally isolated from various organs of advanced patients [16]. FISH analyses were successful on 27 LuCaP lines, representing 22 patients, one of which was also among the metastatic patients described above. These included 27 tumors from 22 patients with *TMPRSS2/ERG* FISH data, 26 tumors from 21 patients with *AR* FISH data, and 25 tumors from 21 patients with *PTEN* FISH data. Together, combining metastatic patient tumors and xenografts derived from advanced-stage prostate cancer patients, the current study evaluated a total of 94 tumors from 32 patients.

Fluorescent In Situ Hybridization (FISH)

TMPRSS2/ERG rearrangement was assessed using our novel 4-color FISH assay as described separately [17]. "*TMPRSS2:ERG*" refers to the presence of fusion of the two genes. "*TMPRSS2/ERG* rearrangement" refers to various subtypes of rearrangement of either or both genes as specified in the Results section. FISH analysis of *AR* gene amplification was performed using the SpectrumOrange AR (Xq12) probe combined with the SpectrumGreen labeled ChrX centromere (Xp11.1-q11.1) CEP X probe as the control (Abbott Molecular, IL). *PTEN* gene deletion was examined using the *PTEN*/CEP10 dual-color FISH Probe set (Abbott Molecular, IL), including the SpectrumOrange labeled PTEN (10q23) probe and the SpectrumGreen labeled Chr10 centromere (10p11.1–10q11.1) CEP 10 probe.

For each sample, a range of 25 to 50 intact and non-overlapping interphase nuclei were enumerated manually using a 100×oil immersion lens on a Zeiss Z1 microscope (Carl Zeiss Canada Ltd, Canada). *AR* gain and *PTEN* deletion were assessed by counting the number of gene signal and the corresponding centromere signal per nucleus. *AR* gain was defined as an average copy number of *AR* per nuclei equal or higher than 2. True *AR* gene amplification was defined as the ratio of the total number of *AR* signals divided by the total number of the X-chromosome centromere equal or greater than 2. Samples with *PTEN* heterozygous deletion had a ratio of the total number of *PTEN* signals divided by the total number of CEP10 signals equal or below 0.75. A *PTEN*/CEP10 ratio equal or below 0.2 is considered homozygous *PTEN* deletion. For patient-level analyses of CRPC patients with multiple tumors, expression by a given marker was considered abnormal if the aberration was seen in at least one tumor.

Expression Array

Agilent 44 K whole human genome expression oligonucleotide microarrays (Agilent Technologies, Inc., Santa Clara, CA) were used to profile prostate cancer xenografts and human castration-resistant soft tissue metastases of prostate. Freshly frozen xenografts were processed to extract total RNA which was amplified one round; patient samples were laser-capture microdissected and amplified two rounds as described previously [18]. Probe labeling and hybridization was performed following the Agilent suggested protocols and fluorescent array images were collected using the Agilent DNA microarray scanner G2565BA. Agilent Feature Extraction software was used to grid, extract, and normalize data. Expression ratios were $\log_2$ scaled and mean-centered across each gene.

Statistical Analysis

To complement the comparisons of archived primary tumor with a separate cohort of patients with metastatic disease, we examined within-patient heterogeneity of *AR* and *PTEN* for patients with metastatic disease, hypothesizing that prostate tumors could differ from contemporaneous metastatic lesions. Linear mixed models with random patient effects were fitted to non-prostate tumors, and a 95% confidence interval calculated for subject-specific [19] predictions of average expression. If a subject's prostate tumor copy number status fell outside the confidence interval, it would be interpreted as evidence of potential differences between the copy number status of primary and metastatic lesions. A linear mixed effects model and the %ICC9 SAS macro was used to calculate intraclass correlation coefficients and their confidence intervals [20]. Logistic regression and generalized estimating equations (GEE) were used to compare rates of abnormality for primary and metastatic samples, controlling for tissue source (rapid autopsy vs xenograft) and within-patient correlation for tumor-level analysis. Heterogeneity of intratumoral variance for different tumor sites was also explored using linear mixed models. Additional statistical inference included Spearman correlation coefficients, and the Wilcoxon rank sum test to compare distributions of the number of markers with abnormal expression. *P*-values were two-sided; statistical analyses were conducted using SAS/STAT software, version 9.3 (SAS Institute, Inc., Cary, NC).

Results

The Prevalence of Genetic Aberrations Detected by the Three-marker FISH Panel in Localized Primary and Metastatic or Castration Resistant (Met/CRPC) Patients

The three-marker FISH panel (Figure 1) used in our study detected frequent genetic aberrations in prostate cancer, and these were significantly more common in Met/CRPC tumors than in untreated primary tumors (Figure 2A).

Of the 34 primary tumors in which all 3 markers could be assessed, 16 (47%) exhibited no aberrations involving *AR*, *PTEN* or *TMPRSS2/ERG*; 11 (32%) were abnormal by one marker only. Six patients' tumors (18%) were detected abnormal by two markers, including 3 with *TMPRSS2*:*ERG* fusion and homozygous *PTEN* deletion, 2 with *TMPRSS2*:*ERG* fusion and heterozygous *PTEN* deletion, and 1 with non-fusion alternative rearrangement along with heterozygous *PTEN* deletion. None of the patients were abnormal by all three markers because there was no detectable *AR* abnormality when the cutoff for *AR* gain was set to $>=2.0$ *AR* per nucleus, an arbitrarily determined stringent cutoff. Two patients would be classified as mild *AR* gain if using *AR* copy number per nuclei $>=1.5$ as the cutoff value, established as mean+3SD based on enumeration results on normal prostate epithelial cells from 18 different samples.

Of the 30 Met/CRPC patients/xenografts with FISH results from all three markers, 4 (13%) had no abnormal marker values. Five (17%) were shown as abnormal by one marker only; 13 (43%) were detected as abnormal by two markers, including 8 (27%) shown as abnormal by *TMPRSS2/ERG* and *AR* FISH and 5 (17%) by *TMPRSS2/ERG* and *PTEN*. Eight patients (27%) were abnormal by all three tests.

We further evaluated subtypes of genetic aberrations detected by each marker in the Met/CRPC cohort (Figure 2 B–D). Rearrangements of *TMPRSS2* and/or *ERG* were detected in 14 patients (47%), including 5 (17%) with the typical single *TMPRSS2*:*ERG* fusion, 5 (17%) with dual or complex *TMPRSS2*:*ERG* fusion, and 4 (13%) with alternative rearrangements without fusion. Copy number increase (CNI) of chromosome 21 was observed in 10 patients (33%) using the *TMPRSS2/ERG* FISH probes. *AR* gain in one or more lesions was observed in 18 patients (60%), including 6 (20%) that resulted from gain of the X-chromosome and 12 (40%) with true *AR* gene amplification ($AR/X >= 2$). Deletion of *PTEN* was detected in 15 patients (50%), including 5 with homozygous deletion.

A Wilcoxon rank sum test suggested that the Met/CRPC cohort ($n = 30$) generally had more alterations detected by FISH than the cohort of primary cancers ($N = 34$) ($W = 1287$, $P<0.001$). *AR* gain, including moderate gain ($W = 1334$, $P<0.001$), and the combination of *TMPRSS2/ERG* and *PTEN* alterations ($W = 1181$, $P = 0.005$) were also significantly more common in the Met/CRPC tumors.

The investigation of individual markers reflected unique trends of changes of each genetic abnormality during the progression of prostate cancer. About 80% of Met/CRPC samples were identified by *TMPRSS2/ERG* FISH as abnormal, compared to 48% in primary samples, and the difference was statistically significant (Table 1; Figure 2B) ($P = 0.03$). This difference appeared to be due to the CNI aberration rather than the *TMPRSS2:ERG* fusion itself; the percentage of patients with fusion or alternative rearrangement remains similar, but the percentage of patients with dual fusion as opposed to single fusion is clearly greater in the Met/CRPC category than in the primary tumor group (Figure 2B). Examining individual tumors (adjusting for within-person correlation and xenograft status), the odds of a Met/CRPC tumor exhibiting an abnormality was 4.5 times greater than odds for a primary tumor ($P = 0.05$). While nearly all primary cancer patients showed normal *AR* status, over 70% of Met/CRPC patients demonstrated various degrees of *AR* gene copy number gain (Table 1; Figure 2C). PTEN FISH showed increased heterozygous *PTEN* deletion and homozygous *PTEN* deletion in Met/CRPC compared with primary patients (Table 1; Figure 2D) ($P = 0.07$ at the tumor level, $P = 0.003$ at the patient level). Of note, for patient-level assessments there was a hierarchy, so if one lesion was heterozygous and the other homozygous, the patient level was considered homozygous.

Data of the entire panel across different individuals showed that prostate cancer patients with *PTEN* deletion also tended to exhibit abnormal results in *TMPRSS2/ERG* FISH (Figure 2E). Among the 34 primary cancer patients with data available from all three markers, 6 of the 8 individuals with *PTEN* deletion (75%) also showed an abnormal *TMPRSS2/ERG* FISH result (Figure 2E). Among the 30 Met/CRPC patients with data available from with either both or all three markers, 13 of the 14 individuals with *PTEN* deletion (93%) also showed abnormalities in *TMPRSS2/ERG* FISH analysis. In Met/CRPC patients, abnormal *TMPRSS2/ERG* FISH results were also more prevalent among patients demonstrating gain of *AR*, and vice versa (Figure 2E). Sixteen out of 17 patients (94%) with *AR* gain showed *TMPRSS2/ERG* abnormalities. Sixteen of 24 patients (67%) with *TMPRSS2/ERG* abnormalities also demonstrated *AR* gain. Detailed FISH results on all metastatic samples from each CRPC patient are summarized in Table 2. Results of xenograft samples are listed in Table 3.

Intra- and Inter-patient Comparison of Genomic Aberrations and Heterogeneity in Castration Resistant Prostate Cancer

The 3-marker FISH analyses yielded two observations from patients with metastatic prostate cancer: (1) within the same patient, aberrations in metastatic tumors were generally consistent across tumors; (2) several primary prostate tumors of CRPC patients exhibited a profile distinct from distant metastatic sites. FISH analyses for *AR* copy number (Figure 3A) and *PTEN*/CEP10 ratio (Figure 3B) showed discordant results between the primary tumors and metastatic lesions. In particular, for patient #9, the prostate tumor showed *AR* copy number increase, whereas the metastatic lesions all had average $AR<2$. For patient #11, the primary prostate tumors showed normal *AR* results while metastatic lesions showed *AR* gain. Similarly, the prostate lesion in patients #3 demonstrated heterozygous *PTEN* deletion when all metastatic lesions had normal *PTEN*. In contrast, for patient #11, the metastatic lesions showed homozygous *PTEN* deletion while the prostate lesion did not. In other cases (#8 and #10), prostate tumors did not differ from metastatic lesions in abnormal *vs* normal marker signals, but were outside of the 95% confidence interval for the subject-specific average based on linear mixed models fit to metastatic lesions.

In general, more than 75% of the variability was between-patient, with relatively little within-patient variation: the intraclass correlation coefficient was 0.76 (95% CI 0.54–0.90) for average *AR* and 0.82 (95% CI 0.62–0.92) for *PTEN*/CEP10. However, when the entire panel was evaluated for each individual, 4 (#3, #5, #9 and #11) out of 8 patients (50%) with data available from all three markers in the local prostate tumors showed different profiles between the primary and metastatic tumors. Further comparison using data of individual markers showed different levels of deviation of the primary from metastatic tumors. Of the 8 patients with available *TMPRSS2/ERG* FISH results on prostate site

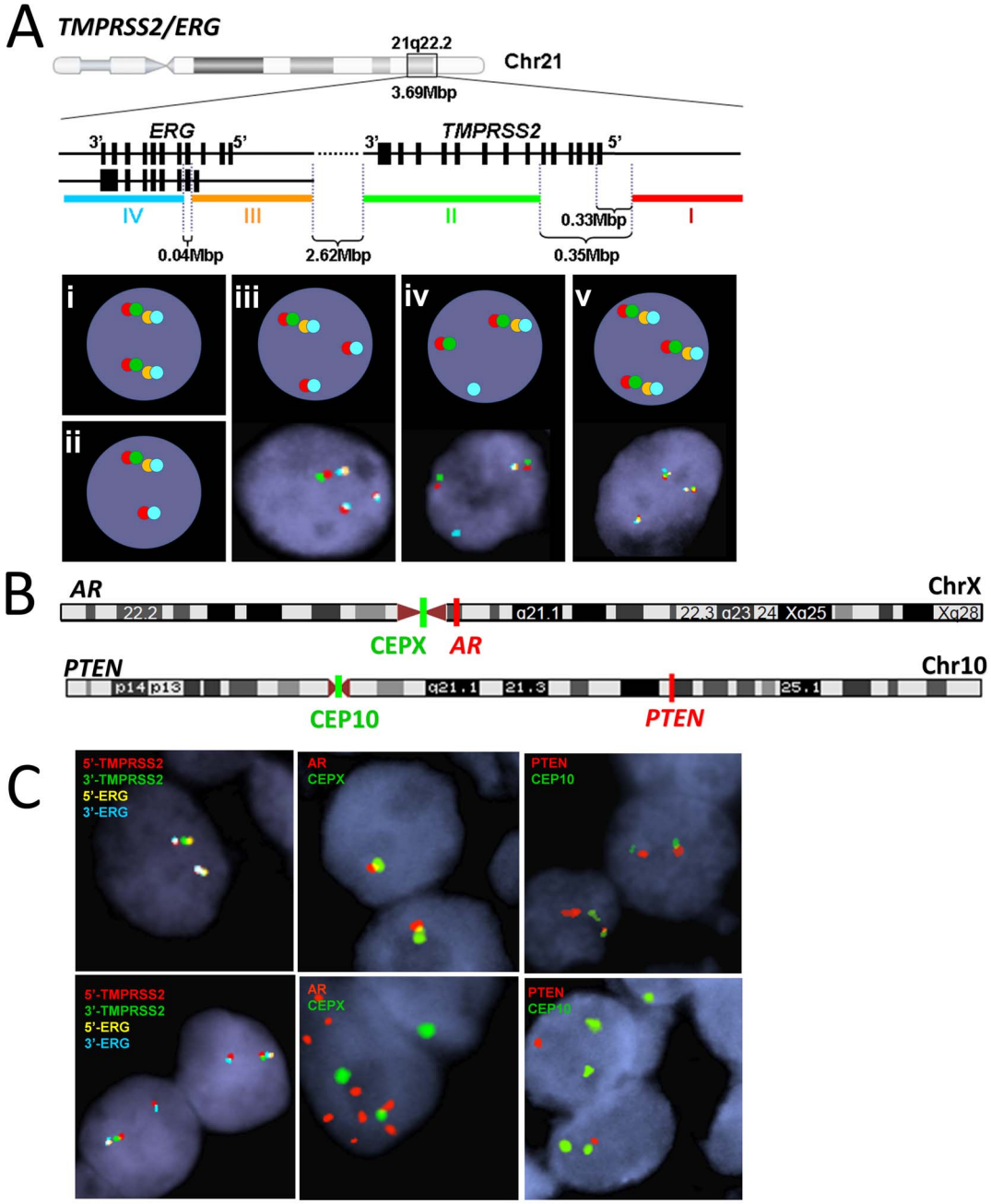

Figure 1. The three-marker FISH panel including *TMPRSS2*/*ERG* rearrangements, *AR* gene amplification, and *PTEN* gene deletion. (A) Illustration of the 4-color FISH technique for the detection of rearrangements of *TMPRSS2* and/or *ERG*. FISH probes target 5′-*TMPRSS2* (red, probe I), 3′-*TMPRSS2* (green, probe II), 5′-*ERG* (gold, probe III), and 3′-*ERG* (blue, probe IV) simultaneously, detecting various signal patterns including normal (i), single fusion(ii), dual/complex fusion(iii), alternative rearrangement without fusion (iv), and copy number increase(CNI) without rearrangements. Captured FISH images of (i) and (ii) are shown in the left panel of 1C; images of (iii) – (v) are shown below the corresponding illustration. (B) FISH probes used to detect *AR* gene amplification and *PTEN* gene deletion *AR* gene amplification was analyzed using probes targeting *AR* (orange) and the X-chromosome centromere (green, CEPX). *PTEN* gene deletion was detected using probes targeting *PTEN* (orange) and the chromosome 10 centromere (green, CEP10). (C) Representative interphase FISH images. Top left, normal *TMPRSS2* and *ERG* signal pattern demonstrating two sets of the four probes per nucleus; Bottom left, *TMPRSS2*: *ERG* fusion shown as juxtaposed red and blue signals concurrent with missing or separation of the interstitial green and gold signals; Top middle, normal *AR* signal pattern demonstrating one orange *AR* and one green X signal per nucleus; Bottom middle, *AR* gene amplification presenting more than twice the number of *AR* signals than the CEPX signals; Top right, normal *PTEN* signal pattern demonstrating 2 orange *PTEN* and 2 green CEP10 signals per nucleus; Bottom right, *PTEN* deletion showing none or 1 copy of *PTEN* signals per nucleus.
doi:10.1371/journal.pone.0074671.g001

tumors, 3 (37.5%) had results in the prostate different from those in other metastatic sites (Table 2). Interestingly, patient #5 demonstrated dual deletion fusion among metastatic sites, while only single deletion fusion was detected in a tumor from the prostate of the same patient. In the analyses of *AR*, 3 (#3, #9, and #11) out of 10 patients (30%) showed results in the prostate that

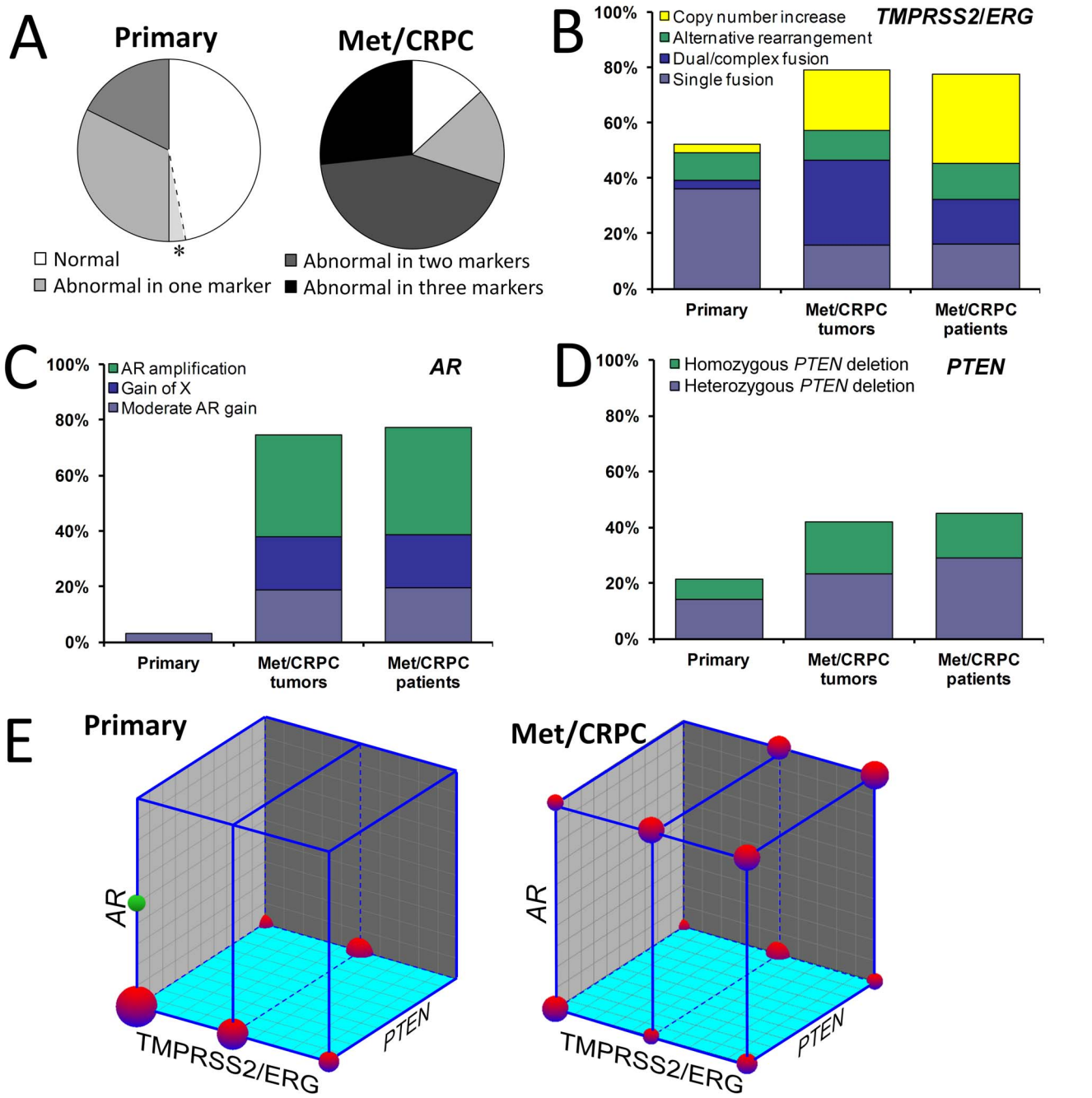

Figure 2. The prevalence of genetic aberrations detected by the panel. A patient with multiple tumors was considered abnormal by a given marker if the aberration was seen in at least one tumor. (A) Pie charts demonstrate the percentage of individuals with no (white), one (light grey), two (dark grey), and three (black) abnormalities detected by the panel among the primary prostate cancer (n = 34) and the metastatic or castration resistant prostate cancer (Met/CRPC) cohort (n = 30), respectively. Among primary patients, an asterisk was used to highlight moderate AR gain (average *AR* per nucleus >= 1.5 but <2). (B-D) Prevalence of each subtype of abnormalities detected by individual FISH marker among the primary patients (one tumor per patient, n = 34), Met/CRPC tumors (n = 81), and Met/CRPC patients/xenografts (n = 30), respectively. *TMPRSS2/ERG* abnormalities are categorized as single fusion (light blue), dual/complex fusion (dark blue), alternative rearrangements (green), and copy number increase (CNI) of the normal gene alleles (yellow). *AR* FISH detected moderate *AR* gain (light blue), gain of X (dark blue) and *AR* gene amplification (green). *PTEN* FISH abnormalities includes heterozygous (light blue) and homozygous (green) *PTEN* deletions. (E) The co-occurrence of abnormalities in the three markers shown as 3D sphere plots for the primary cancer cohort (left) and the Met/CRPC cohort (right). *TMPRSS2/ERG*, *PTEN*, and *AR* results are presented on X, Y, and Z axes, respectively. The value presented on each axis ranges from 0 to 1. "0" denotes normal for a given marker. For *TMPRSS2/ERG*, "0.5" indicates rearrangements, including fusion and alternative rearrangements; "1" means CNI of the normal alleles without any rearrangement. For *PTEN* FISH, both heterozygous and homozygous deletions are presented as "1". For *AR* FISH, "1" indicates *AR* copy number gain (>= 2.0). Patients with the same combination of abnormalities are clustered into a sphere, the volume of which is proportional to the percentage of patients in the respective cohort. Only patients with available data from all three markers are included. The green sphere in the primary patient plot denotes moderate *AR* gain (>1.5 but <2.0).
doi:10.1371/journal.pone.0074671.g002

Table 1. Prevalence of abnormalities detected by each FISH marker among the primary and the metastatic or castration-resistant prostate cancer (Met/CRPC) patients.

	Primary		Met/CRPC		Met/CRPC		*P*value	
	# of patients	%	# of tumors	%	# of patients	%	Tumors[6]	Patients[7]
TMPRSS2/ERG	69		82		31		0.05	0.03
Single fusion	25	36%	13	16%	5	16%		
Dual/complex fusion	2	3%	25	30%	5	16%		
Alternative rearrangement without fusion	4	6%	9	11%	4	13%		
Copy number increase	2	3%	18	22%	10	32%		
Normal	36	52%	17	21%	7	23%		
AR	65		90		31		<0.001	<0.001
Moderate *AR* gain[1]	2	3%	17	19%	6	19%		
Gain of X[2]	0	0%	17	19%	6	19%		
AR amplification[3]	0	0%	33	37%	12	39%		
Normal	63	97%	23	26%	7	23%		
PTEN	42		86		31		0.07	0.003
Heterozygous *PTEN* deletion[4]	6	14%	20	23%	9	29%		
Homozygous *PTEN* deletion[5]	3	7%	16	19%	5	16%		
Normal	33	79%	50	58%	17	55%		

[1]Average *AR* per nucleus ≥1.5 but <2.
[2]Average *AR* per nucleus ≥2 but average AR/X ratio<2.
[3]Average *AR*/X ratio≥2.
[4]Average *PTEN*/CEP10 ratio≤0.75 but >0.2.
[5]Average *PTEN*/CEP10 ratio≤0.2.
[6]Wald tests of abnormal vs. normal for primary vs. CRPC, generalized estimating equations (GEE) with independence autocorrelation, adjusting for rapid autopsy vs xenograft sample for CRPC. Likelihood ratio test for AR (without adjustment for autocorrelation), since no primary samples had abnormal AR.
[7]Wald tests of abnormal vs. normal for primary vs. CRPC, logistic regression adjusting for rapid autopsy vs xenograft sample for CRPC. Likelihood ratio test for AR, since no primary samples had abnormal AR.
doi:10.1371/journal.pone.0074671.t001

deviated from extra-prostatic tumors. The assessment of *PTEN* deletion showed that 2 (#3 and #11) out of 9 patients (22.2%) demonstrated different *PTEN* FISH results between prostate site and metastatic tumors. In patient #11, all extra-prostatic metastasis showed homozygous *PTEN* deletion, while prostate tumors showed normal *PTEN* results. Similarly, the panel data for xenografts also indicated that xenograft lines derived from the same patient tend to show the same genomic abnormality (Table 3).

Intra-tumoral Assessments of Genomic Heterogeneity in Metastatic Patients

We next sought to evaluate variation in genomic alterations detected by the FISH panel in individual cells comprising a primary or metastatic tumor. We found substantial intratumor variation in *AR* copy number for prostate site tumors. Linear mixed models predicted *AR* copy number at the cell level by tumor type, with random patient effects. Table 4 shows estimates for the number of *AR* per cell, and for the covariance parameter estimates that show how within-tumor variation and measurement error differ between tumor types. Prostate site tumors had the highest estimated within-person *AR* standard deviation (1.43 *AR* per cell). Several prostate tumors and lymph node metastasis had some unusually high counts that may have contributed to the estimate. For the *PTEN/CEP10* ratio, the covariance estimates were also found to be heterogeneous by tumor type ($\chi^2_6 = 20$, p = 0.003), but within-patient prostate *PTEN*/CEP10 intratumoral heterogeneity was not different from that of metastasis ($\chi^2_1 = 0.7$, p = 0.40). Table 4 suggests that the tissue-based heterogeneity differences were due to low within-patient variation in the peritoneal and adrenal lesions. These effects may be confounded with patient effects, since few patients had adrenal or peritoneal lesions. By a likelihood ratio test, statistical models with separate covariate estimates for each tumor type fit the data better than a model that did not distinguish between tumors ($\chi^2_6 = 412$, $P<0.001$), and a model that distinguished between prostate tissue and other lesions ($\chi^2_5 = 332$, $P<0.001$).

Correlation of Genomic Alterations and Gene Expression in Castration Resistant Prostate Cancer

In order to investigate the functional relationship of genetic aberrations detected by our panel, we correlated our FISH findings with gene expression data from 91 matching Met/CRPC samples, including 65 patient tumors and 26 xenografts (Table S1).

We first compared *AR* copy number, determined by FISH, with the *AR* transcript abundance, determined by cDNA microarray, from the same tumor sample. We observed a wide range of *AR* expression in Met/CRPC tumors (Figure 4A). The average number of *AR* per nucleus and the level of relative *AR* mRNA were positively correlated with rho = 0.52 ($P<0.001$) (Figure 4A). When normalized to the median *AR* mRNA expression level of all tumors with both *AR* FISH and mRNA expression data (n = 88),

Table 2. FISH data of individual castration resistant metastatic patient tumors.

Patient	Tissue	*TMPRSS2/ERG*	Average *AR* per nucleus	*AR*/*X*	*PTEN*/*CEP10*
8	Liver	Normal	5.50	3.27	1.19
8	LN1	Normal	1.12	1.00	1.04
8	LN2	Normal	4.94	2.74	1.20
8	LN3	Normal	5.70	3.35	1.16
8	Lung	Normal	4.38	2.74	1.12
8	Prostate	Normal	2.52	1.42	1.00
1	Liver	Normal	NA	NA	0.50
1	LN1	Normal	1.00	1.00	0.52
1	LN2	Normal	1.03	1.00	0.49
1	Prostate	Copy number increase	1.00	1.00	0.50
4	Liver	Single fusion	1.19	1.00	0.00
4	LN1	Single fusion	1.05	0.98	0.00
4	Lung1	Single fusion	1.00	1.00	0.00
4	Lung2	NA	1.11	1.00	NA
4	Spleen	Single fusion	1.04	1.00	0.00
4	Prostate	NA	1.08	1.00	NA
5	LN1	Dual/complex fusion	20.37	7.10	0.04
5	LN2	Dual/complex fusion	20.76	6.18	0.05
5	LN3	Dual/complex fusion	37.48	10.18	0.00
5	LN4	Dual/complex fusion	18.16	6.78	0.08
5	LN5	Dual/complex fusion	14.48	6.58	0.10
5	Prostate	Single fusion	102.64	54.60	0.03
2	LN1	Dual/complex fusion	1.10	1.00	1.00
2	LN2	Dual/complex fusion	1.66	0.99	0.80
2	LN3	Dual/complex fusion	1.92	1.02	0.97
2	Lung1	Dual/complex fusion	1.22	1.00	0.96
2	Lung2	Dual/complex fusion	2.00	1.00	0.98
2	Prostate	Dual/complex fusion	1.75	1.00	0.95
9	Adrenal1	Dual/complex fusion	1.62	1.09	1.02
9	Adrenal2	Dual/complex fusion	1.62	1.09	1.02
9	Liver	Dual/complex fusion	1.50	0.99	0.96
9	LN1	Dual/complex fusion	1.86	1.06	0.96
9	LN2	Dual/complex fusion	1.50	0.96	1.00
9	LN3	Dual/complex fusion	1.28	0.98	1.02
9	LN4	Dual/complex fusion	1.26	1.02	0.90
9	Lung1	Dual/complex fusion	NA	NA	0.94
9	Lung2	Dual/complex fusion	1.48	1.04	1.04
9	Spleen	Dual/complex fusion	1.64	1.01	0.86
9	Prostate	Dual/complex fusion	14.22	6.35	0.95
7	LN1	Alternative rearrangement	8.20	3.20	0.73
7	LN2	Alternative rearrangement	16.48	9.81	0.80
7	LN3	Alternative rearrangement	17.32	8.33	0.82
7	LN4	Alternative rearrangement	37.64	12.38	0.50
7	Prostate	Alternative rearrangement	10.20	5.31	0.76
11	LN1	Copy number increase	6.88	3.91	0.03
11	LN2	NA	7.38	4.15	0.05
11	LN3	Copy number increase	7.44	4.33	0.06
11	Lung	NA	5.56	3.39	0.01
11	Prostate	Alternative rearrangement	1.00	1.00	0.94
11	Prostate	Alternative rearrangement	1.10	1.04	1.02
3	Liver	Copy number increase	2.58	1.16	0.94
3	LN1	Copy number increase	2.80	1.32	0.76
3	LN2	Copy number increase	2.88	1.29	0.82
3	Lung	Copy number increase	2.74	1.28	1.00
3	Prostate 1	Normal	4.04	3.61	0.64
3	Prostate 2	Normal	1.32	1.06	NA
6	LN1	Copy number increase	2.56	1.00	NA
6	LN2	Copy number increase	2.44	1.00	0.57
6	LN3	Copy number increase	2.55	1.00	NA
6	Peritoneal	Copy number increase	2.21	0.99	0.45
10	Liver	NA	2.88	1.73	0.51
10	LN1	NA	5.62	3.39	0.44
10	LN2	NA	5.35	3.54	0.51
10	LN3	NA	6.36	3.46	0.50
10	LN4	NA	9.78	5.62	0.50
10	Lung	NA	6.18	3.19	0.47
10	Prostate	NA	9.12	5.36	0.68

Only samples successfully hybridized with at least one marker were presented in the table, including 56 tumors with *TMPRSS2/ERG* FISH, 65 tumors with *AR* FISH, and 62 tumors with *PTEN* FISH results.

doi:10.1371/journal.pone.0074671.t002

samples with *AR* gain (n = 48), including gain of X (n = 17) and *AR* amplification (n = 31) expressed *AR* mRNA at 2.5±0.3-fold (Mean±S.E.) higher than the median, while tumors without *AR* gain (n = 40) had *AR* mRNA level as 0.7±0.2-fold comparing to the median (W = 1106, $P<0.001$). When tumors with *AR* gain were further divided into groups of gain of X (n = 17) vs *AR* gene amplification (n = 31), our data showed that *AR* mRNA was expressed at a similar level between the two (W = 361, $P = 0.24$).

We then assessed the effect of *TMPRSS2*:*ERG* fusion on *ERG* mRNA levels and evaluated whether *ERG* expression also associated with the *AR* abundance in Met/CRPC tumors (n = 80, Figure 4B). Fusion-negative tumors (n = 42) expressed

Table 3. FISH data of individual xenograft tumors.

Xenografts	Tissue	*TMPRSS2/ERG*	Average *AR* per nucleus	*AR/X*	*PTEN/CEP10*
LuCaP81	LN	Normal	1.00	1.00	0.91
LuCaP78	Peritoneal	Normal	1.04	1.00	1.00
LuCaP136	Acites fluid(cells)	Normal	1.04	1.00	0.00
LuCaP153†	NA	Normal	1.50	1.00	1.63
LuCaP147	Liver	Normal	1.96	1.96	1.00
LuCaP49	Omental fat met	Single fusion	1.10	0.97	0.54
LuCaP86.2	Bladder	Single fusion	1.97	1.00	0.93
LuCaP23.12	Liver	Single fusion	2.20	1.04	0.89
LuCaP23.1CR	LuCaP23.1	Single fusion	2.28	1.00	NA
LuCaP23.1	LN	Single fusion	2.48	1.00	0.95
LuCaP35	LN	Single fusion	6.44	2.98	0.91
LuCaP35CR	LuCaP35	Single fusion	34.76	12.78	0.96
LuCaP145.1*	Liver	Single fusion	1.60	1.00	1.15
LuCaP145.2*	LN	Dual/complex fusion	1.79	0.99	0.87
LuCaP93	Prostate	Dual/complex fusion	1.50	0.99	0.00
LuCaP92	Peritoneal	Dual/complex fusion	2.00	1.00	0.90
LuCaP58	LN	Alternative rearrangement	1.52	1.00	0.37
LuCaP96**	Prostate	Alternative rearrangement	1.52	1.03	0.60
LuCaP96CR	LuCaP96	Alternative rearrangement	5.72	3.33	0.79
LuCaP73	Prostate	Copy number increase	1.48	1.00	1.03
LuCaP115	LN	Copy number increase	1.72	1.08	1.02
LuCaP70	Liver	Copy number increase	2.08	1.00	1.00
LuCaP141	Prostate	Copy number increase	2.64	1.00	0.98
LuCaP146	NA	Copy number increase	6.80	3.90	1.16
LuCaP69†	NA	Copy number increase	16.70	7.50	0.53
LuCaP105	Rib	Copy number increase	119.16	70.93	0.61

†Xenograft discontinued.
*Xenograft derived from patient #9 in Table 2.
**Xenograft derived from a patient with localized prostate cancer.
Only samples successfully hybridized with at least one marker were presented in the table, including 23 with *TMPRSS2/ERG* FISH, 26 with *AR* FISH, and 25 xenografts with *PTEN* FISH results.
doi:10.1371/journal.pone.0074671.t003

ERG mRNA at 0.7±0.1 relative to the probe median, while fusion-positive tumors (n = 38) expressed significantly higher *ERG* mRNA at 910.8±3.2 fold relative to probe median (W = 2073, $P<0.001$). Copy number increase (CNI) of *ERG* (or of both *TMPRSS2* and *ERG* without fusion) did not associate with higher *ERG* mRNA expression.

As *ERG* expression in the context of a *TMPRSS2:ERG* fusion is regulated by AR activity, we evaluated the effect of *AR* on *ERG* expression in Met/CRPC tumors with and without *TMPRSS2:ERG* fusion. While both the fusion-positive and fusion-negative samples showed a significant correlation between *AR* mRNA and *ERG* mRNA expression, this correlation appeared stronger in fusion-positive samples (rho = 0.64, $P<0.001$, n = 38) than in fusion-negative samples (rho = 0.36, $P = 0.02$, n = 42). This correlation was further confirmed by a dichotomized comparison of *ERG* expression levels for the 38 fusion-positive samples between low- and high- *AR* mRNA expression groups using the median probe intensity as a divider. The low *AR* expressing tumors (n = 20) expressed *ERG* at 3.6±1.1 fold relative to the probe median, while the high *AR* expressing tumors (n = 18) expressed *ERG* at 21.2±5.8 fold of probe median ($P<0.01$).

Discussion

A Three Marker FISH Panel Detects High Rates of Recurrent Genomic Aberrations in Localized and Metastatic Prostate Cancers

Because of the controversial prognostic utility of *TMPRSS2:ERG* fusion in prostate cancer, we employed the strategy of a three-marker FISH panel to detect well documented prostate cancer DNA aberrations, including *TMPRSS2/ERG* rearrangements, *AR* copy number gain, and *PTEN* deletion. This panel clearly detected a significant number of genetic abnormalities in prostate carcinomas, 53% in primary tumors and 87% in Met/CRPCs. At the individual tumor level, the odds of a Met/CRPC tumor being abnormal were 4.5 times greater than that for a primary tumor. Collectively, if aberrations in these genomic loci associate with aggressive tumor behavior, then this three-marker FISH panel may be a useful tool in distinguishing high-risk patients from low-risk ones at diagnosis or in repeat assessments using active surveillance strategies. In addition, this approach may be particularly useful in characterization of circulating and disseminated tumor cells (CTC/DTC) as using fewer cells for analysis

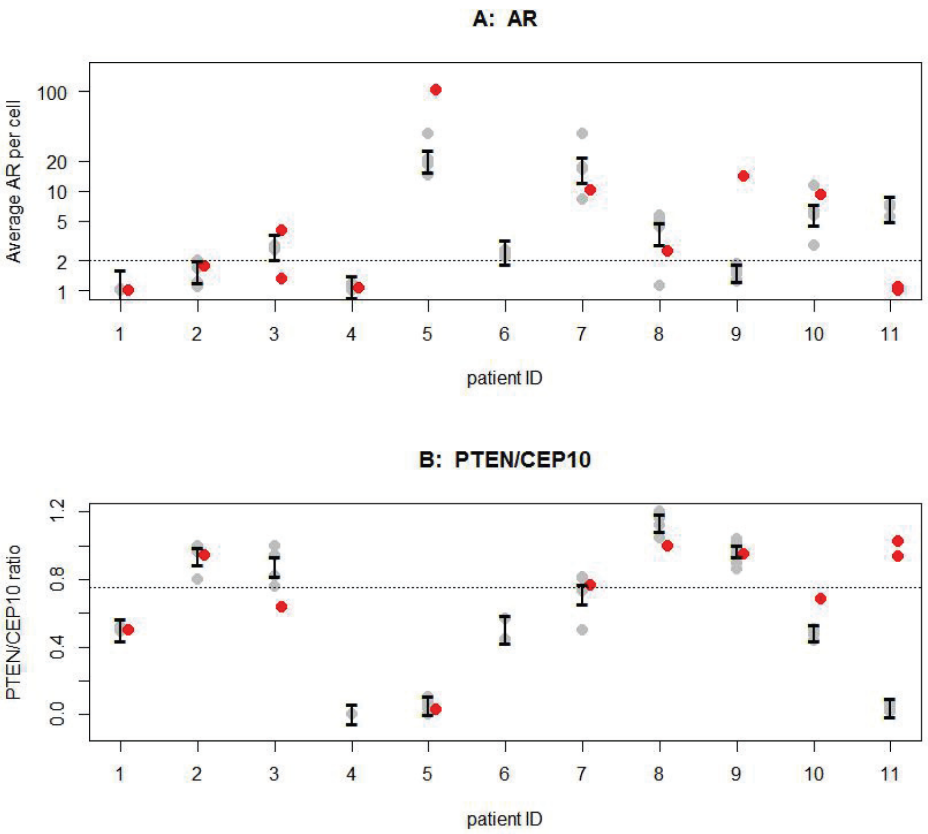

Figure 3. Within-patient heterogeneity of *AR* and *PTEN*/CEP10 for rapid autopsy patients (n = 11). Each tumor's FISH result is represented by a plotting character (grey for metastatic lesions, red for prostate) with multiple lesions in the same patient at the same X coordinate. Confidence intervals for subject-specific average copy number values are shown in black. Thresholds for abnormal signals are marked as horizontal dashed lines on each plot. (A) Average number of *AR* per nucleus. (B) Average *PTEN*/*CEP10* ratio.
doi:10.1371/journal.pone.0074671.g003

Table 4. Summary of intratumoral heterogeneity.

		AR (N = 2591 cells in 11 patients) patients			*PTEN*/*CEP10* (N = 722 cells in 11 patients)		
	N[1]	Average *AR* per cell[2]	Predicted AR per cell (95% confidence interval)	Predicted within-patient standard deviation	Average *PTEN*/*CEP10*[1]	Predicted *PTEN*/*CEP10* (95% confidence interval)	Predicted within-patient standard deviation
Prostate	12	2.1	3.0 (2.6–3.3)	1.43	0.9	0.8 (0.7–0.9)	0.43
Adrenal	2	1.6	1.5 (1.4–1.6)	1.04	1.0	1.0 (0.9–1.1)	0.21
Liver	6	2.6	2.3 (2.1–2.5)	1.12	0.7	0.7 (0.6–0.8)	0.44
Lymph Node	34	5.3	3.5 (3.3–3.7)	1.29	0.5	0.7 (0.6–0.7)	0.47
Lung	10	2.0	2.1 (2.0–2.3)	1.13	1.0	0.7 (0.6–0.8)	0.46
Peritoneal	1	2.2	2.0 (1.7–2.3)	1.06	0.4	0.4 (0.2–0.6)	0.29
Spleen	2	1.3	1.3 (1.2–1.3)	1.02	0.4	0.5 (0.3–0.7)	0.54

[1]Number of tumors in sample.
[2]Median for analyzed tissue.
Predicted values and covariance parameter estimates are from linear mixed models predicting copy number by tumor type, with random patient effects and separate covariance parameter estimates (within-patient heterogeneity and measurement error) for each tumor type.
doi:10.1371/journal.pone.0074671.t004

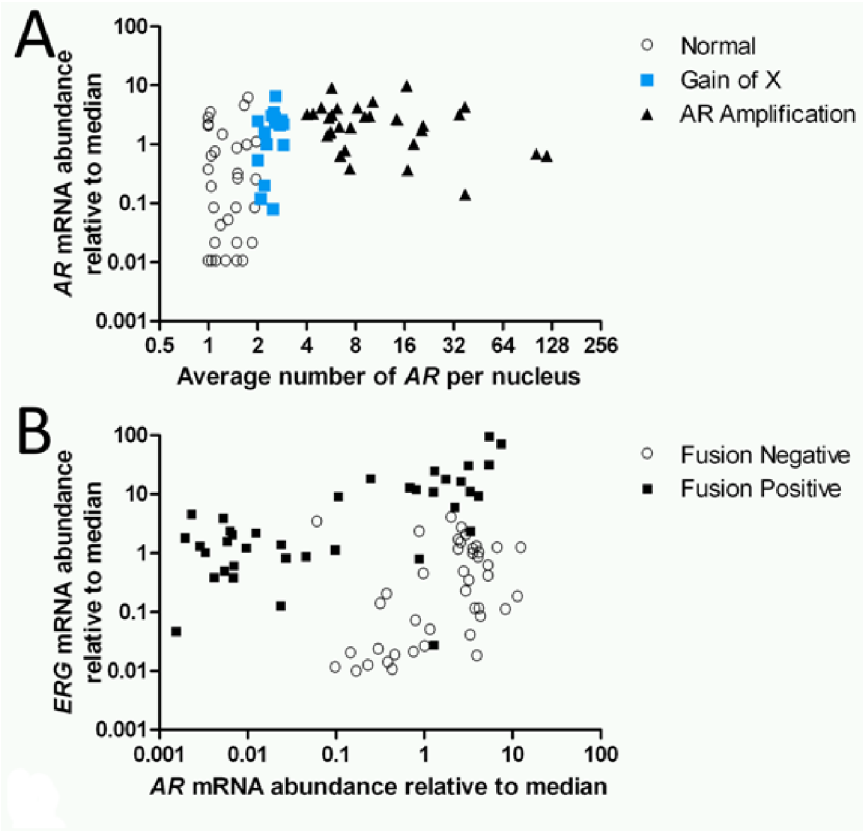

Figure 4. The correlation between changes in gene expression and aberrations detected by the panel. (A) Scatter plot demonstrates the correlation between FISH and expression data of *AR* (n = 88). The X-axis denotes the average number of *AR* signals per nuclei. The Y-axis denotes the *AR* mRNA level detected in the expression array relative to the median. Black open circles denote samples with an average of less than 2 *AR* per nuclei. Blue squares denote samples with copy number gain of *AR* due to gain of X. Black triangles denote samples with *AR* gene amplification. (B) Scatter plot demonstrates the effect of *TMRPSS2*:*ERG* fusion and *AR* expression on the abundance of *ERG* transcript (n = 80). The X- and Y-axis denotes relative mRNA abundance of *AR* and *ERG* compared to the median, respectively. Open circles and filled squares represent tumors without and with *TMPRSS2*:*ERG* fusion, respectively.
doi:10.1371/journal.pone.0074671.g004

and getting data on three specific markers would be a significant advantage. The utility of these three markers is further supported by findings from a recent study using whole exome and transcriptome sequencing technologies [21]. Grasso et al. identified that *AR* and *PTEN* had the highest level of copy number gains and losses, respectively, in prostate cancer, especially CRPC. Their integrated genomic approach also demonstrated the interplay of these genomic alterations with *TMPRSS2*/*ERG* rearrangements. For each individual marker, our study detected similar abnormality rates as reported in the literature. For rearrangements of *TMPRSS2* and/or *ERG*, previous findings showed *ERG* rearrangements in 30–50% of localized prostate cancers [1,2,4,5,22] and 40–50% of metastatic diseases [4,23–25]. With our novel 4-color FISH technique, capable of detecting rearrangements of *TMPRSS2* and/or *ERG* simultaneously in a single hybridization, we found the similar prevalence for *TMPRSS2*:*ERG* fusion, as well as non-fusion alternative rearrangements in 10–12% patients in both groups. However, dual/complex *TMPRSS2*:*ERG* fusion, which has been shown to associate with poor survival, occurs with a substantially greater frequency in Met/CRPC patients (17%) than in primary cancer patients (3%). Similarly, copy number increase (CNI) of *TMPRSS2* and *ERG* without fusion was more frequent in Met/CRPC patients (33%) than in primary cancer patients (3%), suggesting increased genetic instability as the disease progresses, which was also observed in our studies of disseminated tumor cells obtained from prostate cancer patients [23,26].

To date, multiple studies have demonstrated the occurrence of *PTEN* loss ranging from less than 20% to nearly 70% in early stage prostate cancer [8,11,27,28]. The variation could be attributed to multiple factors such as differences in patient populations, cohort sizes, and the cutoffs used to determine the *PTEN* deletion. Setting the cutoffs (based on the percentage of abnormal nuclei among all nuclei scored) as 10% for homozygous and 40% for heterozygous deletion, Reid and colleagues identified 17% of untreated primary prostate cancers exhibiting heterozygous or homozygous deletion of *PTEN* [11]. Setting the cutoffs as 30% for homozygous and 20% for heterozygous deletion, Yoshimoto et al. identified the presence of heterozygous and homozygous *PTEN* deletion in 39% and 5% prostate cancer patients, respectively [8]. We observed *PTEN* deletion in 21% of primary cancer patients and 47% of the CRPC patients based on the average ratio of *PTEN*/CEP 10 signals. Similar to previous findings [29], our study found that *PTEN* deletion tumors also tended to harbor *TMPRSS2*/*ERG* abnormalities (Figure 2E).

Our findings on *AR* gene amplification are unique and particularly interesting. *AR* amplification is generally considered to be only associated with CRPC tumors, induced by hormonal deprivation therapy or treatment with AR antagonists. Previous FISH studies rarely detected *AR* gene amplification in clinically

localized prostate tumors before hormonal therapy, but gain of the X-chromosome has been reported in 30–50% patients when a cutoff for gain was set at 9.8% of all cells examined [30,31], which implied that an average of >= 1.1 copies of the X-chromosome per nucleus were considered abnormal. In recurrent prostate cancer, *AR* amplification was common, with the reported frequency varying between 20% and 60% [6,7,32,33]. In these studies, *AR* gene amplification was defined in a slightly different manner. For example, among the studies that used *AR*/X ratio to define the amplification, the cutoffs vary from 1.5 [32,33], 2.0 [6], to 3.0 [7]. In the present study, we separated the subtype of true *AR* gene amplification, defined as *AR*/X ratio >= 2.0, from general *AR* gain, defined as having an average *AR* per nucleus of >= 2.0. We found *AR* gain in 58% of Met/CRPC patients, including 39% presenting as true *AR* gene amplification and 19% demonstrating *AR* gain due to simultaneous gain of the X-chromosome, with an average number of X-chromosomes per nuclei exceeding 2.0 (Table 1). There was, however, no difference in the *AR* mRNA expression between the groups of X-gain vs *AR* gene amplification; *AR* copy numbers correlated well with *AR* mRNA levels (Figure 3A). We also observed by SNP-array CGH analysis that the multiple X centromere signals observed by FISH sometimes represent only focal gain or amplification of the genomic region around the centromere of the X-chromosome including *AR* rather than gain of the entire X-chromosome (Schoenborn, unpublished data not shown). These data argue for using the absolute *AR* copy number alone to define *AR* gain/amplification in FISH studies regardless of the *AR*/X ratio. Consequently, using the cutoff of 2.0 for *AR* gain would mean that a tumor would be considered abnormal for *AR* gain when *AR* copy number is at least doubled (from one copy in normal male cells to two copies in cancer cells) in 100% of the cells, which might be too stringent a criterion and explains why *AR* gain was never reported previously in primary prostate cancer. Our experimental cutoff based on signal patterns seen in a series of normal controls was 1.48. Therefore, we used the 1.50 cutoff for moderate *AR* gain in Table 1, which translates to that *AR* gain in 50% of the cells would be considered abnormal. With this cutoff, we observed 6% of primary patients and 77% of Met/CRPC patients with *AR* gain. This should be a better definition for *AR* gain and may allow identification of primary prostate cancer patients with high risk for disease progression. Supporting evidence came from LuCaP 96 (Table 3), a xenograft line derived from a localized primary prostate cancer which showed moderate *AR* gain (1.52 *AR* per nucleus). Its castration-resistant derivative line LuCaP 96CR showed clear *AR* amplification (5.72 *AR* per nucleus). The original patient indeed had aggressive disease and died from prostate cancer. The caveat, however, is that the xenograft data may not faithfully represent the original tumor genomics due to potential selection pressures over time on the xenograft specimens.

FISH Detected Genetic Abnormalities Strongly Correlate with Changes at the Expression Level and Suggest Functional Interactions between *AR*, *PTEN* and *TMPRSS2/ERG*

Chaux *et al.* identified a strong association between ERG protein staining using immunohistochemistry and the *TMPRSS2*:*ERG* fusion status defined by FISH [34]. Similarly, our study showed that *ERG* mRNA expression was significantly correlated with the presence of *TMPRSS2*:*ERG* fusion. We also demonstrated a strong positive correlation between *AR* copy number gain and increased level of *AR* mRNA expression, supporting previous studies which showed higher levels of AR protein expression in prostate tumors with *AR* gene amplification than tumors without *AR* amplification [33]. Unlike this study that did not find an effect of X-chromosome gain on *AR* mRNA, we found higher *AR* mRNA levels in tumors with simple gain of X-chromosome, the amplitude of which could not be differentiated from tumors with true *AR* gene amplification. The similarity in *AR* mRNA levels in these two groups may in part be due to the nature of transcriptome array analyses, where the quantification of very high levels of *AR* mRNA reaches a plateau.

Related to the functional interactions of these genetic aberrations, previous studies demonstrated the cooperative relations between *PTEN* deletion and *TMPRSS2/ERG* rearrangements in animal models [29,35]. Clinical studies demonstrated significant correlations between *PTEN* gene deletion and deregulation of p-AKT as well as AR protein expression in advanced localized prostate cancer [9]. Two recent studies suggested cross-talk between androgen signaling pathway and the PI3K signaling in a reciprocal fashion [12,13]. At the genomic level, studies using large clinical cohorts demonstrated both presence and absence of enrichment between *TMPRSS2*:*ERG* fusion and *PTEN* gene deletion in prostate cancer [9,11]. Our study also confirmed enrichment of *TMPRSS2/ERG* abnormalities in tumors with either *PTEN* deletion or *AR* gain (Figure 2E). *AR* gain, but not *PTEN* deletion, was enriched in Met/CRPC tumors with *TMPRSS2/ERG* abnormalities. However, it is not obvious from our study that *PTEN* and *AR* expression were inversely correlated in prostate cancer, as previously reported [14].

More importantly, we demonstrated that *AR* and *ERG* expression levels strongly correlated with each other, especially in *TMPRSS2:ERG* fusion-positive tumors (Figure 4B). We propose the model that moderate *AR* gain in a *TMPRSS2:ERG* fusion-positive primary prostate cancer might synergistically enhance the expression of *ERG*, which gives growth advantage to those cells with moderate *AR* gain. *ERG* expression beyond a certain threshold would convey castration resistance to the tumor cells, which in turn increases the *AR* copy number and expression to compensate for androgen deprivation, contributing to disease progression and metastasis. Future work is needed to further study the hypothesis and the prognostic utility of the three-marker FISH panel.

Heterogeneity of Genetic Aberrations Detected by the Three-marker FISH Panel

The genetic heterogeneity assessment among CRPC patients showed that the major variability were between-patient. Within a given CRPC patient, aberrations in metastatic tumors were generally consistent across tumors, which are congruent with the general notion that metastatic cancer cells originated from the primary cancer cells and, therefore, likely maintain the same genetic lesion. However, some primary tumors may differ from metastatic lesions (Figure 3). This observation supported previous findings which demonstrated that primary prostate cancer is multiclonal, but most prostate cancer metastases are likely monoclonal in origin [23,36]. Also, primary tumors in the CRPC patient population have been exposed to aggressive therapy, which over time could result in genomic alterations inconsistent with the original primary tumor. In addition, intra-tumor variation was evident by both the *AR* and *PTEN* markers, which showed greater heterogeneity from tumors at the prostate site than distant metastases. This does not negate the significant intra-patient protein expression observed in our previously reported studies [37]. These findings support the multifocal and possibly multiclonal nature of advanced stage prostate cancer, especially at the prostate microenvironment [38].

In summary, we evaluated both primary cancer patients and Met/CRPC patients for the presence of *TMPRSS2/ERG* rearrangements, *AR* gene copy number gain, and *PTEN* deletion using a three-marker FISH panel. Our panel detected highly recurrent genetic abnormalities that showed distinct distribution between primary prostate cancer patients and Met/CRPC patients. Since these abnormalities occurred more frequently in Met/CRPCs, which represent more aggressive disease, when present in localized primary prostate cancer, would convey aggressive characteristics to these localized tumors. Therefore, our results support the prognostic potential of the three-marker FISH panel for risk stratification. FISH findings strongly correlated with the transcriptome levels and provided further insight in the interaction of these three gene related functional pathways. Tumor heterogeneity analysis demonstrated more inter-patient variability than intra-patient, and that the intra-patient tumor heterogeneity was mainly due to the deviation of the prostate site tumor from metastases. Future studies will focus on applying this panel to retrospective or prospective studies on untreated primary cancer patients and on CTC/DTC to test its ability to stratify patients and predict clinical outcome.

Supporting Information

Table S1 Shows the mRNA expression results of *AR* and *ERG* of all Met/CRPC tumor samples used in this study.
(DOCX)

Acknowledgments

Our special deep thanks to Barbara Trask, Ph.D. for her tremendous support for this study. We also thank Eva Corey, Ph.D., Colm Morrisey, Ph.D., and Larry True, M.D., for their roles in the rapid autopsy and xenograft generation program.

Author Contributions

Conceived and designed the experiments: XQ MF. Performed the experiments: XQ GR CF LG IC MF. Analyzed the data: XQ GR CF BFK EM CSH CP RV PSN MF. Contributed reagents/materials/analysis tools: EM CSH CP RV PSN MF. Wrote the paper: XQ MF BFK IC EM RV PSN. Critical review of the manuscript: GR CF LG CSH CP.

References

1. Tomlins SA, Rhodes DR, Perner S, Dhanasekaran SM, Mehra R, et al. (2005) Recurrent fusion of TMPRSS2 and ETS transcription factor genes in prostate cancer. Science 310: 644–648.
2. Attard G, Clark J, Ambroisine L, Fisher G, Kovacs G, et al. (2008) Duplication of the fusion of TMPRSS2 to ERG sequences identifies fatal human prostate cancer. Oncogene 27: 253–263.
3. Clark JP, Cooper CS (2009) ETS gene fusions in prostate cancer. Nat Rev Urol 6: 429–439.
4. Gopalan A, Leversha MA, Satagopan JM, Zhou Q, Al-Ahmadie HA, et al. (2009) TMPRSS2-ERG gene fusion is not associated with outcome in patients treated by prostatectomy. Cancer Res 69: 1400–1406.
5. Esgueva R, Perner S, C JL, Scheble V, Stephan C, et al. (2010) Prevalence of TMPRSS2-ERG and SLC45A3-ERG gene fusions in a large prostatectomy cohort. Mod Pathol 23: 539–546.
6. Visakorpi T, Hyytinen E, Koivisto P, Tanner M, Keinanen R, et al. (1995) In vivo amplification of the androgen receptor gene and progression of human prostate cancer. Nat Genet 9: 401–406.
7. Bubendorf L, Kononen J, Koivisto P, Schraml P, Moch H, et al. (1999) Survey of gene amplifications during prostate cancer progression by high-throughout fluorescence in situ hybridization on tissue microarrays. Cancer Res 59: 803–806.
8. Yoshimoto M, Cunha IW, Coudry RA, Fonseca FP, Torres CH, et al. (2007) FISH analysis of 107 prostate cancers shows that PTEN genomic deletion is associated with poor clinical outcome. Br J Cancer 97: 678–685.
9. Sircar K, Yoshimoto M, Monzon FA, Koumakpayi IH, Katz RL, et al. (2009) PTEN genomic deletion is associated with p-Akt and AR signalling in poorer outcome, hormone refractory prostate cancer. J Pathol 218: 505–513.
10. Yoshimoto M, Joshua AM, Cunha IW, Coudry RA, Fonseca FP, et al. (2008) Absence of TMPRSS2:ERG fusions and PTEN losses in prostate cancer is associated with a favorable outcome. Mod Pathol 21: 1451–1460.
11. Reid AH, Attard G, Ambroisine L, Fisher G, Kovacs G, et al. (2010) Molecular characterisation of ERG, ETV1 and PTEN gene loci identifies patients at low and high risk of death from prostate cancer. Br J Cancer 102: 678–684.
12. Carver BS, Chapinski C, Wongvipat J, Hieronymus H, Chen Y, et al. (2011) Reciprocal feedback regulation of PI3K and androgen receptor signaling in PTEN-deficient prostate cancer. Cancer Cell 19: 575–586.
13. Mulholland DJ, Tran LM, Li Y, Cai H, Morim A, et al. (2011) Cell autonomous role of PTEN in regulating castration-resistant prostate cancer growth. Cancer Cell 19: 792–804.
14. Wang Y, Romigh T, He X, Tan MH, Orloff MS, et al. (2011) Differential regulation of PTEN expression by androgen receptor in prostate and breast cancers. Oncogene 30: 4327–4338.
15. Morrissey C, True LD, Roudier MP, Coleman IM, Hawley S, et al. (2008) Differential expression of angiogenesis associated genes in prostate cancer bone, liver and lymph node metastases. Clin Exp Metastasis 25: 377–388.
16. Corey EV, R. (2007) Xenograft Models of Human Prostate Cancer. In: Chung LWK IW, amd Simons JW, editor. Contemporary Cancer Research: Prostate Cancer: Biology, Genetics, and the New Therapeutics. Totowa: Humana Press. pp. 3–31.
17. Qu X, Randhawa G, Friedman C, O'Hara-Larrivee S, Kroeger K, et al. (2013) A novel four-color fluorescence in situ hybridization assay for the detection of TMPRSS2 and ERG rearrangements in prostate cancer. Cancer Genet 206: 1–11.
18. Sharma A, Yeow WS, Ertel A, Coleman I, Clegg N, et al. (2010) The retinoblastoma tumor suppressor controls androgen signaling and human prostate cancer progression. J Clin Invest 120: 4478–4492.
19. Zeger SL, Liang KY, Albert PS (1988) Models for longitudinal data: a generalized estimating equation approach. Biometrics 44: 1049–1060.
20. Hankinson SE, Manson JE, Spiegelman D, Willett WC, Longcope C, et al. (1995) Reproducibility of plasma hormone levels in postmenopausal women over a 2–3-year period. Cancer Epidemiol Biomarkers Prev 4: 649–654.
21. Grasso CS, Wu YM, Robinson DR, Cao X, Dhanasekaran SM, et al. (2012) The mutational landscape of lethal castration-resistant prostate cancer. Nature 487: 239–243.
22. FitzGerald LM, Agalliu I, Johnson K, Miller MA, Kwon EM, et al. (2008) Association of TMPRSS2-ERG gene fusion with clinical characteristics and outcomes: results from a population-based study of prostate cancer. BMC Cancer 8: 230.
23. Holcomb IN, Young JM, Coleman IM, Salari K, Grove DI, et al. (2009) Comparative analyses of chromosome alterations in soft-tissue metastases within and across patients with castration-resistant prostate cancer. Cancer Res 69: 7793–7802.
24. Mehra R, Tomlins SA, Yu J, Cao X, Wang L, et al. (2008) Characterization of TMPRSS2-ETS gene aberrations in androgen-independent metastatic prostate cancer. Cancer Res 68: 3584–3590.
25. Perner S, Demichelis F, Beroukhim R, Schmidt FH, Mosquera JM, et al. (2006) TMPRSS2:ERG fusion-associated deletions provide insight into the heterogeneity of prostate cancer. Cancer Res 66: 8337–8341.
26. Holcomb IN, Grove DI, Kinnunen M, Friedman CL, Gallaher IS, et al. (2008) Genomic alterations indicate tumor origin and varied metastatic potential of disseminated cells from prostate cancer patients. Cancer Res 68: 5599–5608.
27. Verhagen PC, van Duijn PW, Hermans KG, Looijenga LH, van Gurp RJ, et al. (2006) The PTEN gene in locally progressive prostate cancer is preferentially inactivated by bi-allelic gene deletion. J Pathol 208: 699–707.
28. Yoshimoto M, Cutz JC, Nuin PA, Joshua AM, Bayani J, et al. (2006) Interphase FISH analysis of PTEN in histologic sections shows genomic deletions in 68% of primary prostate cancer and 23% of high-grade prostatic intra-epithelial neoplasias. Cancer Genet Cytogenet 169: 128–137.
29. King JC, Xu J, Wongvipat J, Hieronymus H, Carver BS, et al. (2009) Cooperativity of TMPRSS2-ERG with PI3-kinase pathway activation in prostate oncogenesis. Nat Genet 41: 524–526.
30. Gallucci M, Merola R, Leonardo C, De Carli P, Farsetti A, et al. (2009) Genetic profile identification in clinically localized prostate carcinoma. Urol Oncol 27: 502–508.
31. Gallucci M, Merola R, Farsetti A, Orlandi G, Sentinelli S, et al. (2006) Cytogenetic profiles as additional markers to pathological features in clinically localized prostate carcinoma. Cancer Lett 237: 76–82.
32. Brown RS, Edwards J, Dogan A, Payne H, Harland SJ, et al. (2002) Amplification of the androgen receptor gene in bone metastases from hormone-refractory prostate cancer. J Pathol 198: 237–244.
33. Ford OH, (2003) Androgen receptor gene amplification and protein expression in recurrent prostate cancer. J Urol 170: 1817–1821.
34. Chaux A, Albadine R, Toubaji A, Hicks J, Meeker A, et al. (2011) Immunohistochemistry for ERG expression as a surrogate for TMPRSS2-ERG fusion detection in prostatic adenocarcinomas. Am J Surg Pathol 35: 1014–1020.

35. Carver BS, Tran J, Gopalan A, Chen Z, Shaikh S, et al. (2009) Aberrant ERG expression cooperates with loss of PTEN to promote cancer progression in the prostate. Nat Genet 41: 619–624.
36. Liu W, Laitinen S, Khan S, Vihinen M, Kowalski J, et al. (2009) Copy number analysis indicates monoclonal origin of lethal metastatic prostate cancer. Nat Med 15: 559–565.
37. Roudier MP, True LD, Higano CS, Vesselle H, Ellis W, et al. (2003) Phenotypic heterogeneity of end-stage prostate carcinoma metastatic to bone. Hum Pathol 34: 646–653.
38. Lindberg J, Klevebring D, Liu W, Neiman M, Xu J, et al. (2012) Exome Sequencing of Prostate Cancer Supports the Hypothesis of Independent Tumour Origins. Eur Urol.

Pritchard PCF Abstract 2013

MSH2 and _MSH6_ Structural Rearrangements in Hypermutated Microsatellite Unstable Advanced Prostate Cancer

Colin C. Pritchard[1], Colm Morrissey[2], Akash Kumar[3], Xiaotun Zhang[2], Christina Smith[1], Ilsa Coleman[4], Stephen Salipante[1,3], Jonathan F. Tait[1], Robert Vessella[2], Tom Walsh[5], Jay Shendure[3], and Peter S. Nelson[4]

[1]Department of Laboratory Medicine, University of Washington, Seattle WA; [2]Department of Urology, University of Washington, Seattle WA; [3]Department of Genome Sciences, University of Washington, Seattle, WA; [4]Division of Human Biology, Fred Hutchinson Cancer Research Center, Seattle, WA; [5]Division of Medical Genetics, Department of Medicine, University of Washington, Seattle, WA.

Background: A hypermutated subtype of advanced and lethal prostate cancer was recently described in about 15% of patients (Kumar et al. 2011), but mechanisms that lead to hypermutation in prostate cancer have not been characterized. We hypothesized that mutations in DNA repair pathway genes lead to hypermutation.

Methods: We identified hypermutated cases using exome sequencing in advanced and lethal prostate cancer samples from two sources: LuCaP xenograft, and and metastatic specimens obtained from the rapid autopsy program at the University of Washington. We then interrogated 30 DNA repair pathway genes in hypermutated and non-hypermutated cases using a targeted deep sequencing approach that included capture of intronic and flanking DNA sequences. We developed a custom bioinformatics pipeline to accurately detect structural variation, copy number variation, and insertion/deletion mutations of all sizes. Immunohistochemisty (IHC) and microsatellite instability (MSI) PCR testing were performed using standard methods.

Results: We performed deep sequencing of DNA repair pathway genes on 23 LuCaP xenografts, including 3 hypermutated tumors LuCaP 58, LuCaP 73, and LuCaP 147. All three hypermutated tumors had complex structural rearrangement mutations in *MSH2*, *MSH6* or both genes, while only 1 of 20 non-hypermutated tumors had structural rearrangements in these genes (LuCaP 145.1, derived from a patient with neuroendocrine prostate cancer). A second loss-of-function mutation in *MSH2* or *MSH6* was detected in the three hypermutated tumors, but not in LuCaP 145.1, supporting bi-allelic gene inactivation in the hypermutated tumors. *MSH2* and *MSH6* are mismatch DNA repair genes that act together as a heterodimer, and bi-allelic inactivating mutations of either gene are predicted to result in miscrosatellite instability. MSI-PCR on the 3 hypermutated LuCaP xenografts confirmed they were each microsatellite unstable. IHC for DNA mismatch repair proteins in hypermutated tumors demonstrated complete loss of MSH2 and/or MSH6 in a pattern consistent with the inactivating mutations detected by sequencing, and intact MLH1 and PMS2 expression in all cases. Non-hypermutated tumors were microsatellite stable and had intact MSH2 and MSH6 protein, except LuCaP 145.1, which exhibited heterogeneous loss of MSH6 protein. For hypermutated xenograft LuCaP 147 we obtained 4 different metastatic sites from the patient from whom the xenograft line was derived and found that the same complex *MSH2* structural rearrangements were present in all 4 metastatic sites, including bone, and were absent in non-tumor tissue.

Conclusions: Complex structural rearrangements in mismatch DNA repair genes *MSH2* and *MSH6* are a major mechanism underlying hypermutation in advanced prostate cancer and result in microsatellite instability.